FACULTY OF INFORMATION TECHNOLOGY AND ELECTRICAL ENGINEERING
DEGREE PROGRAMME IN WIRELESS COMMUNICATIONS ENGINEERING

MASTER'S THESIS

CHARACTERISTICS OF AGGREGATED TRAFFIC IN LORAWAN

Author	Muhammad Asad Ullah
Supervisor	Assist. Prof. Dr. Hirley Alves
Second Examiner	Assist. Prof. Konstantin Mikhaylov

May 2020

Asad Ullah M. (2020) Characteristics of Aggregated Traffic in LoRaWAN. University of Oulu, Faculty of Information Technology and Electrical Engineering, Degree Programme in Wireless Communications Engineering, Master's Thesis, 52 p.

ABSTRACT

Over the past few years, internet-of-Things (IoT) request a large number of smart devices to communicate and exchange information without direct human assistance. As the number of IoT nodes are increasing rapidly, the massive machine-type communication (mMTC) in 5G enables us to integrate the IoT massive traffic and applications without affecting the traditional services. Low-Power Wide-Area Networks (LPWAN) are emerging commercially and considered as fundamental enablers of IoT, Industrial Internet-of-Things (IIoT), and industrial revolution 4.0 because of their license free frequency bands, long range, low power consumption, and low cost. In recent years, LoRaWAN is appearing as one of the most leading LPWAN technologies. The main contribution of this work is examining the characteristics and modeling the aggregated traffic of a large and dense LoRa Network that is deployed as a monitoring system inside Tellus Innovation Arena, University of Oulu, with the concept of IoT-based digital campus as a Wireless Access IoT service of 5GTN. To understand the traffic behaviour, we analysed the inter-arrival times of the transmissions for different weeks, days, and hours. The statistical presentation of data reveals that the trend of transmissions is exponential, that shows that most of the transmissions were within the inter-arrival time of less than 10 seconds while few of them have inter-arrival time over 20 seconds. After that, we fitted inter-arrival times into the exponential distribution, which helped us to find the mean inter-arrival time of the 5GTN traffic which is further used for the modeling of aggregated traffic. Finally, we performed the transmission compression from a gateway to the Network Server that will be beneficial to efficiently utilize the resources and bandwidth. The results demonstrate that the proposed aggregation mechanism increases the system goodput.

Keywords: 5GTN, LPWAN, Internet-of-Things, LoRa, Traffic modeling

TABLE OF CONTENTS

FOREWORD

This thesis mainly focuses on the statistical characteristics of 5GTN LoRa packets transmissions and the modeling of aggregated traffic. This research work was completed at Centre for Wireless Communications (CWC) under MOSSAF project. First of all, I would like to express my sincere gratitude to my mentor and supervisor Assist. Prof. Dr. Hirley Alves for giving me opportunity to be part of MTC group and providing me platform to polish my research skills. I am thankful to him for always being supportive and providing guidance throughout this work that gave me the directions to accomplish the target results of this work.

A very special thanks goes to Arliones Hoeller for always being available to guide me as well as for our research collaborations. Thanks for being a part of my journey, nice discussions and good suggestions. I would also like to thank Jean De Souza Santana for his valuable feedback.

Furthermore, I am thankful to Irfan Muhammad and Ibrahim Shahzad for showing me positive side of Oulu and encouraging to join University of Oulu. I am also thankful to Rumana Yasmin for providing me 5GTN LoRa traffic data to carry out this research work. I would also like to thank all of my colleagues working in MTC group for always organizing different activities and maintaining supportive work environment, special thank goes to Fahad Qasmi for all the assistance during my thesis. Next, I would like to thank Idris Badmus and Junnaid for all the moments and memories which we shared in office.

Back in Pakistan, I would like to express my gratitude to my teachers Shibli Nisar and Fawad Khan, Ibrahim Khan, Khalil Ullah, Usman Abbasi and Tariq Rahim. I would like to thank my parents and siblings for their supports and love throughout my educational journey. I dedicate this work to my best friend and elder brother Abdul Rehman for always being my mentor in all the matters of my life and motivating me towards my research passion.

Oulu, 11th May, 2020

Muhammad Asad Ullah

LIST OF ABBREVIATIONS AND SYMBOLS

BW	Bandwidth
CO_2	Carbon dioxide
CR	Coding rate
CRC	Cyclic Redundancy Check
G	Goodput
l_i, l_{i+1}	Inner and Outer radii of i-th annulus, respectively
N_P	Number of Aggregated Packets
N_{P^*}	Optimal Number of Aggregated Packets
R_b	Bit Rate
R_S	Symbol Rate
SF	Spreading Factor
T_S	Symbol duration
μ	Mean inter-arrival time
λ	Arrival rate

3GPP	Third Generation Partnership Project
4G	Fourth Generation of Mobile Communication Systems
5G	Fifth Generation of Mobile Communication Systems
5GTN	5G Test Network
ACK	Acknowledgment
API	Application Programmable Interface
ARQ	Automatic Repeat Request
CDMA	Code Division Multiple Access
CRC	cyclic redundancy check
CSS	Chirp Spread Spectrum
D-BPSK	Differential Binary Phase-shift Keying
dB	Decibel
dBm	Decibel-milliwatts
DL	Downlink
DR	Data Rate
DSSS	Direct Sequence Spread Spectrum
E2E	End-to-End
eMBB	Enhanced mobile broadband
ETSI	European Telecommunications Standards Institute
FEC	Forward Error Correction
FHDR	Frame Header
FRMPayload	Frame Payload
GSM	Global System for Mobile Communications
H2H	Human to Human communication
HTTP	HyperText Transfer Protocol
IEEE	Institute of Electrical and Electronics Engineers
IoT	Internet-of-Things
IIoT	Industrial Internet-of-Things
IP	Internet Protocol

ISM	Industrial, Scientific and Medical
LoRaWAN	LoRa Wide Area Network
LPWAN	Low Power Wide Area Network
LTE	Long-Term Evolution
LTE-A	Long Term Evolution Advanced
MAC	Media Access Control
MHDR	MAC Header
MIC	Message Integrity Check
mMTC	Massive Machine-type Communication
MQTT	Message Queuing Telemetry Transport
MTC	Machine-type communications
NB	Narrowband
NFV	Network Function Virtualization
NS	Network Server
PHY	Physical Layer
QoS	Quality of Service
QPSK	Quadrature Phase Shift Keying
RPMA	Random Phase Multiple Access
SDN	Software Defined Network
SNR	Signal to Noise Ratio
TCP	Transmission Control Protocol
ToA	Time-on-Air
UE	User Equipment
UL	Uplink
URLLC	ultra-reliable low latency communication
UDP	User Datagram Protocol
WSN	Wireless Sensor Network

1 INTRODUCTION

The Internet-of-Things (IoT) is the integration of modern electronic devices, smart sensors, internet protocols, and wireless communications technologies. In last decade, IoT has gained huge popularity among researchers, industrial sectors and various other fields. Its applications are rapidly gaining popularity in many domains such as industrial operations [1], smart parking [2], healthcare [3], smart cars [4], smart homes [5], and smart campus [6]. IoT systems comprise user smart devices, sensors and actuators, that are able to connect and exchange information with each other without or with limited human assistance. For instance, the utilization of IoT in smart healthcare (e-health) will deliver fast, safe and effective services. Similarly, Industrial Internet-of-Things (IIoT) technologies are available for security, control, monitoring and management applications in industrial sectors. According to a Gartner Inc. report, there will be around 26 billion IoT devices deployed worldwide by 2020 [7]. In the Statista report, it is predicted that there will be over 75 billion IoT devices worldwide by 2025 [8]. In [9], authors have divided IoT enablers into three layers; smart systems, connectivity solution and analytics. Figure 1 demonstrates these three major enablers of IoT.

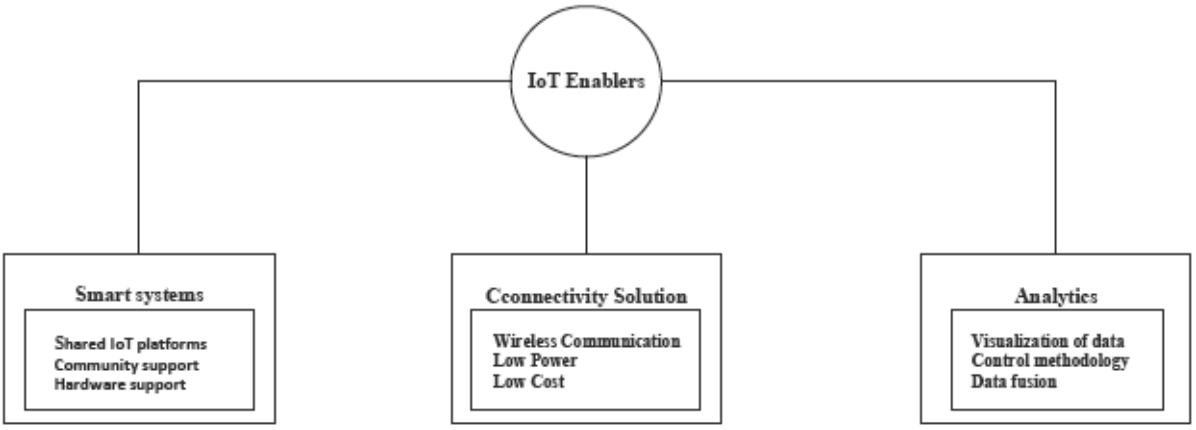

Figure 1. IoT Enablers: smart systems, connectivity solutions, and analytic (sense-making).

The smart system layer is responsible for shared IoT platforms, supportive software and hardware platforms. This layer is involved in data acquisition. In smart systems, community support plays an essential role in decreasing the development cost for IoT applications because of online available tutorials and software libraries. Analytical decision making is also one of the enablers for IoT applications. It handles the visualization of sensors data, control methodologies and multi-modal data fusion approaches. The most important IoT enabler, connectivity solution deals with the transmission of data through the wireless communication between the sensors and the user devices, which should be economical in terms of power consumption and cost. In IoT market, LPWAN technologies, namely LoRa, Sigfox and NB-IoT are emerging for large-scale IoT deployment [10]. Unlike Sigfox, LoRa technology is based on Chirp Spread Spectrum (CSS) modulation that provides robustness against interference [11]. A study shows that LoRaWAN consumes ten times lesser energy as compared to NB-IoT to transmit same payload because NB-IoT implies a lot of signalling overhead (other control

packets) for establishing the connection and scheduling the resources [12]. In this thesis work, we present LoRa aggregation mechanisms that transmit the aggregated packets from gateway to Network Server (NS). As a result, it increases the network goodput, and will significantly help to reduce the number of transmissions and packet overhead because of aggregation.

1.1 Machine-type communications

In telecommunications, Machine-type communications (MTC) has revealed several benefits in terms of reducing the network deployment cost and expanding the coverage area. MTC defined as the exchange of information between embedded systems, computers, smart sensors, IoT devices, actuators and mobile devices without or with limited human assistance [13, 14]. The wireless communication and networking technologies Zigbee, XBee, IEEE 802.15.4 and LPWAN are used in MTC communication. The exchange of data in MTC devices can be controlled through various networks such as multi-hop networks, point-to-point (P2P) and star topology. The ad hoc and mesh networks have been observed as the source to provide internet connection to smart devices.

The Fourth Generation of Mobile Communication Systems (4G) cellular networks (LTE and LTE-Advance) have bring many services for handling MTC data traffic but primarily these telecommunication networks are basically designed for the human to human (H2H) communication. On contrary, the traffic of MTC systems have different characteristics than H2H traffic which leads to create troubles in servers of core networks (CNs) and radio access and the congestion issues [15]. The MTC services and applications are very significant to the future adaptation and success of Fifth Generation of Mobile Communication Systems (5G) [16]. A typical MTC architecture is illustrated in Figure 2.

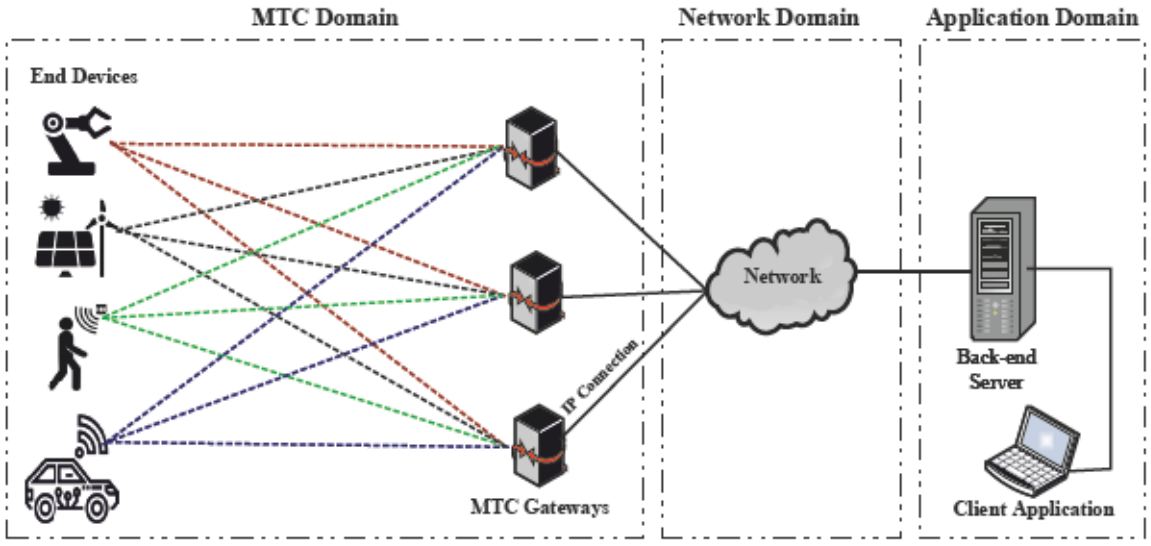

Figure 2. Network architecture of machine-type communications (MTC).

MTC domain comprises various kinds of smart devices, sensors and actuators which are connected with MTC gateway through MTC Network area (e.g. Bluetooth). MTC gateway provides a communication connection between the MTC devices and the Network in network domain. In the application domain the data is analysed, and it performs specific operations.

The support of MTC is considered as a main innovation for 5G deployment. It will help to increase the throughput, enhancement of coverage area, and long battery lifetime. It will also decrease the end-to-end (E2E) delay and ability to support a large number of smart devices [17].

The most of MTC applications worked under the domain of IoT. The growth of MTC and IoT are open doors for green initiatives such as smart cities, smart homes and green buildings. MTC is also playing a major role in public and private sector automation [18]. In [19], MTC is considered as a major enabler of smart cities technologies and the authors also represented MTC based standards and protocols for the smart cities. They have divided the smart cities architecture into three parts; data exchange, configuration management and MTC device management. The open research challenges of MTC are low bandwidth consumption, low cost, low power consumption, massive MTC traffic, quality of services (QoS) provisioning, wide coverage area, security and privacy challenges [20]. Researchers are hopeful to overcome these challenges in the future.

1.2 Traffic characteristics and modeling

IoT traffic characteristics determine the pattern of transmissions behavior in a network, and it is an essential prerequisite for various applications. As a fact, the behavior of IoT and MTC traffic depends on the type of service and application deployment scenarios. In general, IoT traffic patterns are classified as either periodic, event-based or a combination of both. The periodic traffic is the pattern of transmitting the information data with the constant intervals. On the other hand, event-based traffic does not follow a consistent pattern, instead, the transmissions depend on external events [21].

We studied several scientific works focusing on the insights of traffic flow for IoT use cases. In [22], the authors present a survey of traffic classification in IoT networks. Traditionally, port-based approaches use packet headers for classification, i.e. web traffic is identified with TCP port 80. As a drawback, it has only 30%-70% accuracy. Payload-based classification not only considers headers of the packets but also uses data for the decisions. This approach is also known as packet-based classification, and another name is Deep Packet Inspection (DPI). As like port-based classification, it is also used to identify the type of traffic (HTTP, FTP and SMTP). The complexity of payload-based classification is high, that leads to higher computational costs.

Moving towards the advance approaches, statistical classification method performs the analysis using data mining techniques from machine learning algorithms to determine the statistical attributes and patterns of the IoT traffic [23]. Some example of statistical characteristics of IoT traffic are packet length, packet duration, inter-arrival time, and traffic flow idle time. This method overcomes the shortcomings of port-based and packet-based classifications because it avoids the examination of packet contents. Another technique known as behavioral classification discovers the application types by observing all traffic that is received at hosts [24]. It analyzes the pattern of traffic shape, peak load,

and volume. Another literature presents the network traffic characteristics (regular, irregular, and infrequent) of IoT use cases such as smart building, smart healthcare, smart environment, smart city, smart transportation and smart agriculture [25]. In MTC paradigm, the device types are extremely heterogeneous that includes wearable devices, utility meters, environmental sensors and many other unforeseen applications. A large dense city scenario with 10,000 houses per km^2 was used for massive IoT application use cases. These applications used the devices such as water, electricity, and gas meters, position monitor of the rental bikes, accelerometers of cars to observe the driver behavior and vending machines [26]. Thus, Table 1 summarizes the traffic characteristics of IoT devices for smart city scenarios.

Table 1. Traffic characteristics of IoT devices for smart city scenario.

	Water Meters	**Electricity Meters**	**Gas Meters**	**Vending Machines**
Packet Size	100 bytes	100 bytes	100 bytes	150 bytes
Packet interval	12 hours	24 hours	30 minutes	24 hours
Device density	$10{,}000/km^2$	$10{,}000/km^2$	$10{,}000/km^2$	$150/km^2$

Motivated by the fact that IoT and MTC traffic behavior depends on the application scenarios, we perform the statistical classification to understand the characteristics of a LoRaWAN based real monitoring system. The University of Oulu Smart Campus has a large and dense LoRaWAN network containing 331 nodes constantly monitoring several sensors such as temperature, luminosity, and CO_2 [27]. Ideally, each device is configured to transmit 96 packets daily with the constant interval of 15 minutes. Although, the traffic pattern of these nodes should be periodic but during sensor node to gateway communication the losses and collisions could affect the pattern of traffic. Also, sensors are transmitting LoRa packets over the three communication channels (868.10 MHz, 868.30 MHz, and 868.50 MHz) and selection of these channels is random for transmission. Lets consider a scenario, when one of these channels goes down or experience high packet losses then it is not possible to theoretically understand the traffic pattern for accurate modeling. That is why it is very essential to study the behavior of actual traffic of network with the help of statistical analysis. One of the contributions of this thesis work is to solve such problem by analysing the traffic characteristics of real-life use case to determine the accurate traffic patterns and mean inter-arrival time (μ), which is further used for aggregated traffic modeling.

Network behavior analysis and traffic modeling are essential to understand the influence of IoT applications and for the optimization of a network. The characteristics of IoT and MTC traffic differ greatly from conventional cellular communication. MTC applications request low power consumption measures. On the other hand, traditional H2H network has flexible energy requirements because of the ability to recharge. IoT and MTC networks traffic are tend to be dominant in uplink. To design a IoT uplink traffic model, it is important to grasp the deep understanding of the characteristics of its traffic. Conventionally, most of IoT traffic model are based on assumptions that the statistical behavior of data generation is either standard poisson process or exponential distribution, without the actual experimental evidence [28, 29, 30].

The work in [31] fills this gap by IoT traffic modeling based on an actual data of smart home automation system. Their experimental setup contains a single sensor node that

comprises different sensors including temperature, touch, motion, light, and image sensor module. These sensors are connected with Raspberry Pi, which is further linked with the Central Processing Unit (CPU) through a USB WiFi adaptor. On the other hand, our aggregated traffic model is based on an actual large dense IoT network [27]. To the best of authors' knowledge, this work is the first one that deals with the traffic characterization and modeling of large dense LoRaWAN deployment for the 5G test network.

1.3 Data Aggregation in MTC

In typical communication systems the size of metadata (control information) is negligible as compared to the payload. Conversely, in MTC applications, most of the traffic is generated from the sensors in form of short packets with metadata may be of the same size as the actual intended message. In this case, the packet overhead is significant and demands for optimized design. Figure 3 shows a packet format with metadata and data for long and short packets.

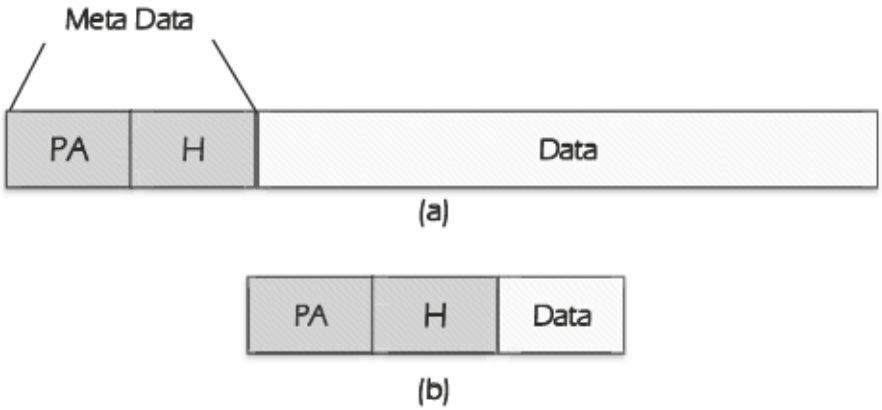

Figure 3. Packet structure with metadata and data. Typically, metadata comprises the header (H) and preamble (PA). (a) Long data packet format (b) MTC short data packet generated by sensors.

Data aggregation plays a vital role in improving the overall efficiency of large-dense connectivity. It is the key solution technique to acquire, aggregate and communicate the data efficiently to reduce the traffic congestion, transmission overhead and increase the network goodput [32]. In massive connectivity scenario, typically sensors transmit the data directly to the destination and it could be excessive for the receiver to process the data accurately. Hence, data aggregators collect the data from the large deployment of sensors and aggregate the data packets at an intermediate node. After that, it forward the aggregated data packets to the receiver. Moreover, the aggregation helps to reduce the number of packet transmissions on the gateway to NS link. In a MTC use case, where several gateways share the same medium to connect with the NS. In such scenario, aggregation approach could reduce interference and collision probability as well. Figure 4 depicts the typical aggregation mechanism.

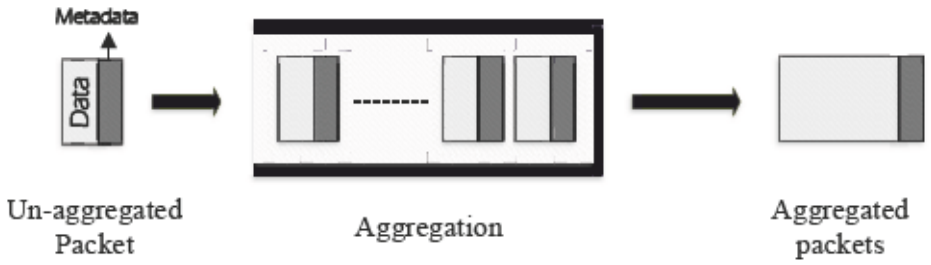

Figure 4. The diagram of typical data aggregation mechanism.

Note that the MTC devices have different delay requirements depending on the application scenario. The fixed data aggregator (FDA) decrease overhead and the number of transmissions from aggregator to destination at the cost of additional communication delay [33]. For delay sensitive use cases, priority-based data aggregation methods can be use at gateway that successfully maintains a good trade-off between the overhead and delay requirement [34]. To make data aggregation more efficient, it is essential to understand the characteristics of the traffic in the network that is why we performed the statistical analysis to study the pattern and mean inter-arrival time of 5GTN LoRaWAN traffic.

1.4 LoRa gateway message forwarding protocol

LoRaWAN comprises three main elements: *end-devices* that are connected via a single-hop to one or several *gateways*, which is further connected with a *Network Server (NS)* through an IP connection [35]. For instance, gateway has the option to use a cellular connection to communication with a NS, or it can be a Wi-Fi medium. Furthermore, it can also use Ethernet port to connect with NS through a wired infrastructure [36]. In IP network, two widely used protocols are User Datagram Protocol (UDP) and Transmission Control Protocol (TCP). Semtech LoRaWAN uses UDP as a packet forwarding protocol from gateway to NS [37]. By using it, applications can transmit information as datagrams to hosts on the IP network. In case of UDP, the prior communication is not needed to set up data paths or the channels for communications. It is based on a connectionless communication model with a few protocol mechanisms. UDP supports checksum, port numbers for source and destinations of the datagram.

The communication is done without handshaking and without a guarantee of transmissions and ordering. UDP is suitable for the applications without error detection and correction codes, it avoids the protocol stack overhead. UDP is mostly used in time sensitive applications. Its header is 8 bytes and the range for the port numbers is from 0 to 65535, while the port number 0 is booked. These port numbers are beneficial to identify the different users requests. UDP headers have 2 bytes long source port and the destination port has the same length. UDP length and checksum are also 2 bytes for each. UDP header packet structure is depicted in Figure 5.

Our work also contributes by the LoRa packets aggregation at the gateway. The proposed aggregation mechanism waits for a specific numbers of packets, then it transmits the aggregated packets from the gateway to the NS using the UDP protocol. The aggregation process increases gateway to NS level goodput and reduces transmission

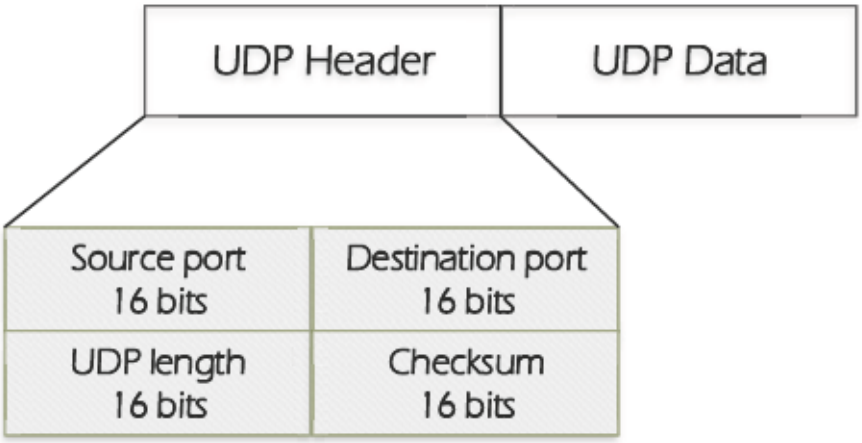

Figure 5. Packet structure of UDP protocol.

overhead at the trade-off with extended communication delay because of queuing. In our case, we opted for UPD as Semtech (packet forwarder protocol) did because it does not add extra delays. UDP structure is simple and offers higher processing capability, it is faster than TCP. As a shortcoming, its reliability is low as compared to TCP because UDP does not check whether it has delivered the data to the receiver or not. UDP just keeps on sending the messages regardless of the ACK. UPD application scenarios using few packets per transaction will be unlikely to undergo reliability issues. On the other hand, TCP continuously look over the ACKs to make the communication reliable, its transmission process becomes slower. In this regard, we preferred UDP to avoid further delays.

The design of communication protocol between the gateway and NS is very basic. It does not authenticates the gateway or NS. The acknowledgements are responsible for accessing the quality of a network, but not to correct the losses of UDP datagrams. For upstream message flow, the gateway transmits the PUSH_Data message that carries the data packets being transferred to the LoRaWAN NS. After receiving the PUSH_Data message, NS responds to the gateway with a PUSH_ACK message, which holds the information about sequence number accommodated in the PUSH_DATA message. The gateway does not respond to the lost PUSH_ACK message [38]. PUSH_DATA message includes extended unique identifier (EUI), JSON is JavaScript object notation, and it is text-based technique of denoting the name and value pairs. It only contains ASCII characters. Figure 6 demonstrates the LoRaWAN upstream gateway message flow diagram.

Traditionally, at a time, gateway can only do one transmission [39] that is why our approach aggregate the LoRa packets up to N_P, after that gateway send these aggregated packets to the NS in a single transmission that is beneficial in term of efficiently utilizing the resources.

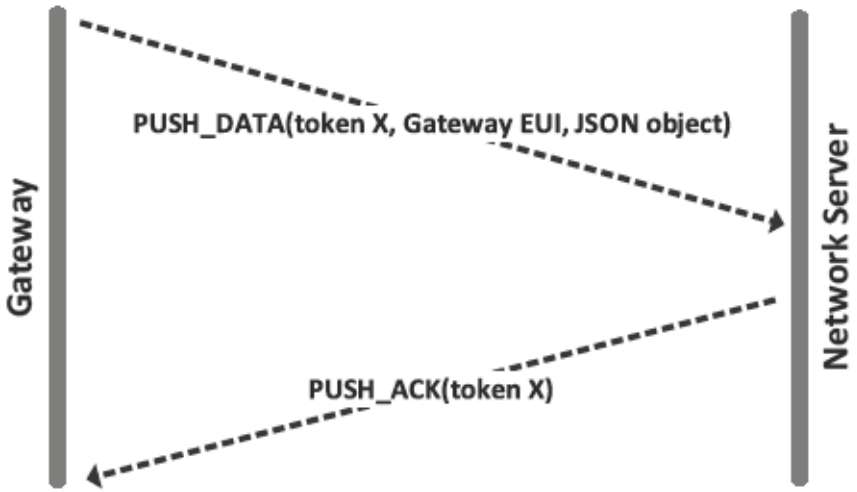

Figure 6. Upstream gateway message protocol sequence representation.

1.5 Thesis contribution

Most of the existing IoT traffic models are lacking the experimental evidence. With this goal in mind, this thesis work present the traffic modeling of actual LoRaWAN network. We examine the statistical characteristics of 5GTN LoRa Network, which is deployed in Tellus Innovation Arena, University of Oulu as monitoring system with the concept of IoT based digital campus. There are in total 331 LoRa sensor nodes which are monitoring motion, CO_2, amount of light, temperature and humidity. The statistical analysis shows that the traffic behavior of inter-arrival times of transmissions is exponential. After that, we fitted the mean inter-arrival time into the exponential distribution to model the aggregated traffic of 5GTN LoRaWAN. Furthermore, our work also contributes by a aggregation mechanisms and optimization of the packet forwarding protocol that result into improvement of network goodput. Normally, gateway transmits the packet whenever it receives from the sensor node. Unlike the traditional technique, in our scheme, the gateway aggregates the packets then it transfer to the NS. The motivation behind aggregation of packets is that it could be used to significantly reduce transmission overhead and collisions of large scale IoT applications. To the best of authors knowledge, no work has been done to modeled the accurate traffic of LoRaWAN based on the real data collected from the LoRa sensor nodes. Therefore, our results can be a significant contribution for the researchers and engineers to deeply understand the characteristics of real-world LoRaWAN based monitoring systems.

1.6 Thesis Outline

The remaining of this thesis is structured as follow:

- **Chapter 2:** discusses and compares the characteristics of different existing LPWAN technologies: Sigfox, RPMA, Weightless, and NB-IoT.

- **Chapter 3:** presents the detailed overview of LoRa PHY, LoRaWAN, and their packet formats. It also touches the LoRaWAN network architecture and its protocol structure.
- **Chapter 4:** provides the details of 5GTN and deployment of LoRaWAN as a concept of digital campus. It also presents the 5GTN LoRa traffic characterization, aggregated traffic modeling and limitations of the proposed aggregation mechanism.
- **Chapter 5:** concludes this thesis work and presents the ideas for the future work.

2 LOW-POWER WIDE-AREA NETWORKS (LPWAN)

In this chapter, we discuss some available LPWAN technologies and their characteristics. In the modern era, the spectacular growth and transformation of wireless connectivity are driven by the IoT paradigm, with technologies having attributes of large-scale network infrastructure with low-cost sensors connected to the Internet. In this context, LPWANs are popular in terms of prototypes, standards, and on the commercial level because of their significance regarding power efficiency along with long range [40]. Within this context, LoRa, SigFox, NB-IoT, Weightless, RPMA and DASH7 [41]

2.1 LPWAN technologies for IoT connectivity

LPWAN are suitable for smart devices that transmit a small amounts of data packets over a long distance with the requirement of energy efficiency. Bluetooth, Wifi, and Zigbee communication have a limited range, while LPWAN has the communication range exceeding several kilometers. Several technologies including LoRa, Sigfox, Weightless and Igenu are under the umbrella of LPWAN and most of them use unlicensed band, 868 MHz ISM in Europe and 915 MHz ISM in US [42]. The most commonly used IoT wireless technologies are Bluetooth, Zigbee, RFID, wireless sensor networks (WSNs)/wireless ad hoc networks. These technologies are mainly for short range communications, with limited coverage area and specific applications. LPWAN technologies are divided into two categories, Ultra Narrow Band (UNB) and Wide-band based on the modulation scheme. UNB uses the narrow-band communication channels with a lower bandwidth of 25 kHz. The wide-band uses a higher bandwidth of 125 kHz to 250 kHz and uses spread spectrum multiple access approaches to manage the several users in one channel [41]. Figure 7 illustrates the comparison of different wireless technologies in terms of range and power consumption. Table 2 shows the characteristics of the LPWAN technologies.

Table 2. Comparison of characteristics of LPWAN technologies.

	LoRaWAN	**Sigfox**	**RAMP**	**NB-IoT**
Battery life	10+ years	10+ years	20+ years	10+ years
Modulation	CSS	D-BPSK	DSSS (UL) CDMA (DL)	QPSK
Frequency band	subGHz ISM	subGHz ISM	2.4 GHz ISM	Licensed LTE
UL peak rate	50 kbps	100 bps	-	230 kbps
DL peak rate	50 kbps	600 bps	-	230 kbps

Figure 8 considers the many factors including cost, QoS, latency, payload size, range, coverage and deployment for the comparison of NB-IoT, LoRa and Sigfox. It is concluded that each one of these LPWAN technologies has their own benefits. LoRa and Sigfox outperform NB-IoT in terms of cost, capacity and battery life. Meanwhile, NB-IoT is advantageous in concern of QoS and latency [43].

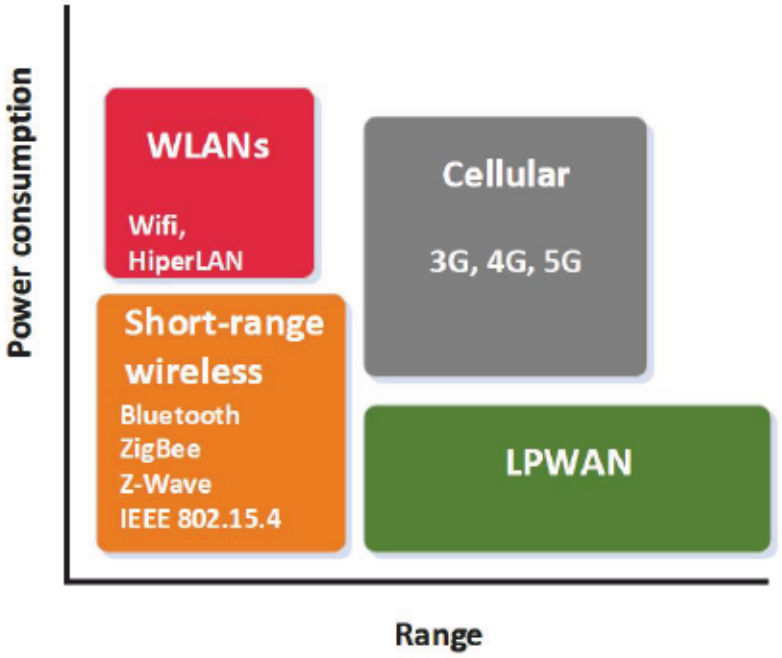

Figure 7. Comparison of range and power consumption of different wireless technologies.

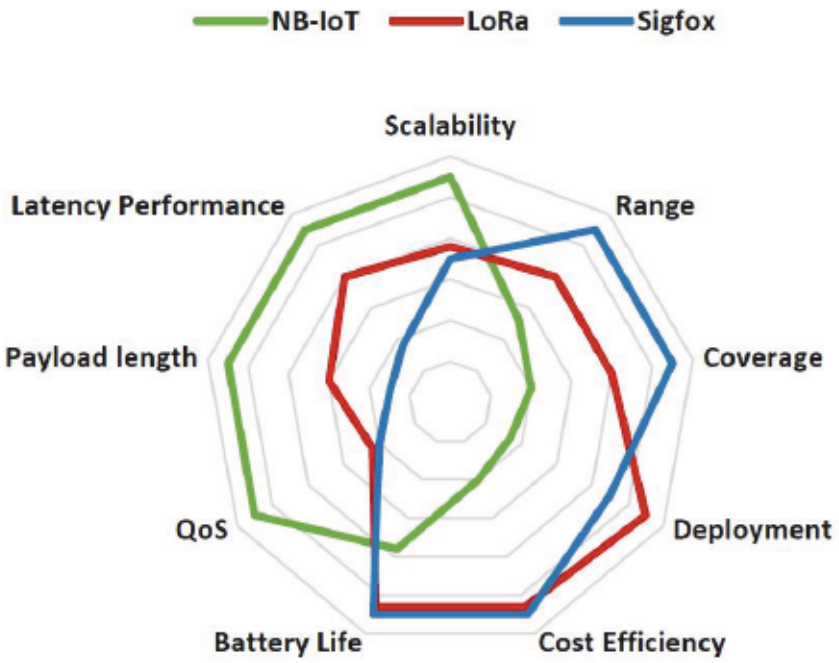

Figure 8. Comparison of LoRa, Sigfox, NB-IoT in terms of IoT factors.

2.1.1 Sigfox

Sigfix is the first LPWAN technology introduced in the market in 2009 and has been emerging since then. Sigfox uses differential binary phase-shift keying (D-BPSK) with

a fixed bandwidth and being sent with a rate of 100 bps in Europe and 600 bps in the United States. The benefits of D-BPSK modulation is that it brings a great efficiency in the spectrum medium access and made it easy for the implementation. The duty cycle limitations for Sigfox are restricted to 0.1% to 10% because of regional restrictions. In the European region, the transmit power is limited to 14 dBm. The practical implementation of Sigfox forms star topology. Sigfox has centralize and simple network architecture, the nodes can communicate directly with the base station [44]. Each base station can supports up to a massive number of end-devices within a communication range of 3-10 km for the urban area or 30-50 km in rural areas. In 2019, the Sigfox technology coverage is available in 65 countries. The technology major standards are based on the principles of providing minimal channel for transmission of small data that would aggregate with the other protocols such as 3G, 4G, 5G, WiFi, Bluetooth etc. Scheduling a back-up communication channel for the worst-case scenario when the main communication links goes down. Moreover, Sigfox provides a strong network security for the different applications. As a LPWAN technology, it reduces the power consumption of the network and the node can transmit for the decades with the same battery. The communication stack of Sigfox is demonstrated in Figure 9.

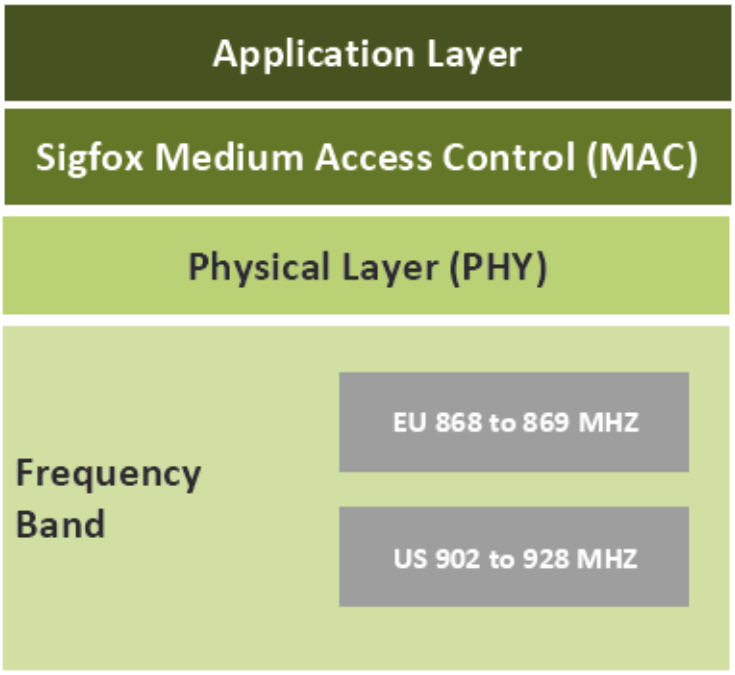

Figure 9. Sigfox protocol stack.

Communication channel exists under the radio frequency layer, and the physical layer is responsible for the modulation schemes. In order to make the communication robust, data is transmitted with redundancy up to 3 times on the multiple channels at the different time interval to gain the frequency and time diversity.

2.1.2 Random Phase Multi Access (RPMA)

Random Phase Multi Access (RPMA) is one of the Ingenu LPWAN technology. RPMA has low network cost, long battery life, a high network capacity, and a low endpoint cost. It has over 100 kbytes per day throughput for the smart meters. To provide reliability, it also has an efficient acknowledgement structure. RPMA provides downlink capability for a large dense network containing a wide range of devices, which is needed to update configurations, activating functions, or to deliver data that the nodes requires to perform specific operations. Moreover, RPMA has a variety of packet sizes different devices that require flexible packet size can use that option. In contrast to other LPWAN technologies, RPMA works on 2.4 GHz band. It also has the ability to operate over the long-range wireless connections and challenging environments because of its effective physical layer design. It mainly focused on smart grid applications [45]. In fact, RPMA in the essence is an ad hoc network, where nodes retransmit the data packets of each other.

2.1.3 Weightless

Weightless technology provides LPWAN connection for IoT applications. It can work in both sub-1 GHz licensed and license exempt spectrums. The Weightless Special Interest Group (SIG) activities include managing ideal disputes, providing an open standard for the IoT device connectivity, innovation, and up-gradation of the standards. It delivers competitive benefits over the alternative in the Third Generation Partnership Project (3GPP) space in local area networks (LAN) space and also across the emerging LPWAN space. In addition, it delivers a distinction of capacity, cost, open standards, range, QoS, security, energy consumption and reliability [41, 46]. Weightless offers the data rates from 0.625 kbps to 100 kbps. Typically, a Weightless node works on a transmit power of 14 dBm up to 30 dBm. It connects these nodes with the base station through star topology.

2.1.4 Narrowband-IoT

Narrowband-IoT also known as NB-IoT (inaugurated in 3GPP Release 13) is a radio access system developed from the current LTE functionalities with some optimization and simplifications. It can coexist with LTE as well as with Global System for Mobile Communications (GSM) under the umbrella of licensed frequency bands [47]. Compared to LTE, NB-IoT uses a smaller spectrum of 180 kHz in the physical layer. In downlink, 12 subcarriers are used and each subcarrier has 15 kHz spacing to occupy the total 180 kHz bandwidth. In uplink mode, NB-IoT also has an option to use 3.75 kHz subcarrier spacing with 48 subcarries to cover the bandwidth of 180 kHz. This numerology can be achieved by expanding time domain four times to keep it compatible with LTE. NB-IoT allows three different operation modes, as depicted in Figure 10.

In stand-alone operation mode, NB-IoT uses the frequency bands of GSM. For guard-band operations, it consumes the unused resource blocks of the LTE carrier's guard band. Finally, the NB-IoT operation mode that uses the resources within a LTE carrier is known as in-band operation [48].

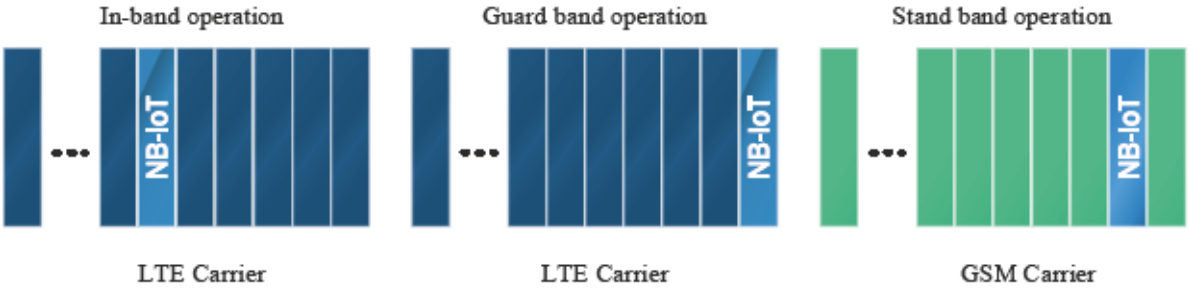

Figure 10. Operation modes for NB-IoT.

In contrast to LoRa and Sigfox, the deployment of NB-IoT has a high deployment cost. Moreover, deployment of NB-IoT is not suitable for regions that do not have LTE connectivity [43]. For instance, NB-IoT is not a wireless connectivity solution for smart agriculture applications. NB-IoT is primarily designed for indoor coverage, large dense deployment, low power consumption, and also for the MTC applications that demand small bursts but several transmissions. Table 3 shows the uplink (UL) and downlink (DL) channels, with their usages.

Table 3. NB-IoT channels and their usages [48].

Channels		Responsibility
DL	Narrowband Physical Downlink Control Channel (NPDCCH)	UL and DL scheduling information
	Narrowband Physical Broadcast Channel (NPBCH)	Master details for the system access
	Narrowband Physical Downlink Shared Channel (NPDSCH)	DL allocated and common data
	Narrowband Synchronization Signal (NPSS/NSSS)	Frequency and time synchronizations
UL	Narrowband Physical Random Access Channel (NPRACH)	Random access
	Narrowband Physical Uplink Shared Channel (NPUSCH)	UL dedicated data

3 AN OVERVIEW OF LORA

LoRa is based on spread spectrum modulation technique that is the derivative of CSS modulation and it trades the data rate for the sensitivity using a constant channel bandwidth. It applies a flexible data rate, uses orthogonal spreading factors that enables the system to trade data rate for the power consumption or communication range, to improve the performance of the network in a fixed bandwidth. LoRa is the PHY layer, sometimes the term is also used to denote a combination of LoRa PHY and LoRaWAN. LoRa PHY utilizes unlicensed ISM band and uses CSS radio modulation approach. On the other hand, LoRaWAN is protocol stack at network and media access control (MAC) layers [49]. Figure 11 depicts the communication protocol stack of LoRaWAN.

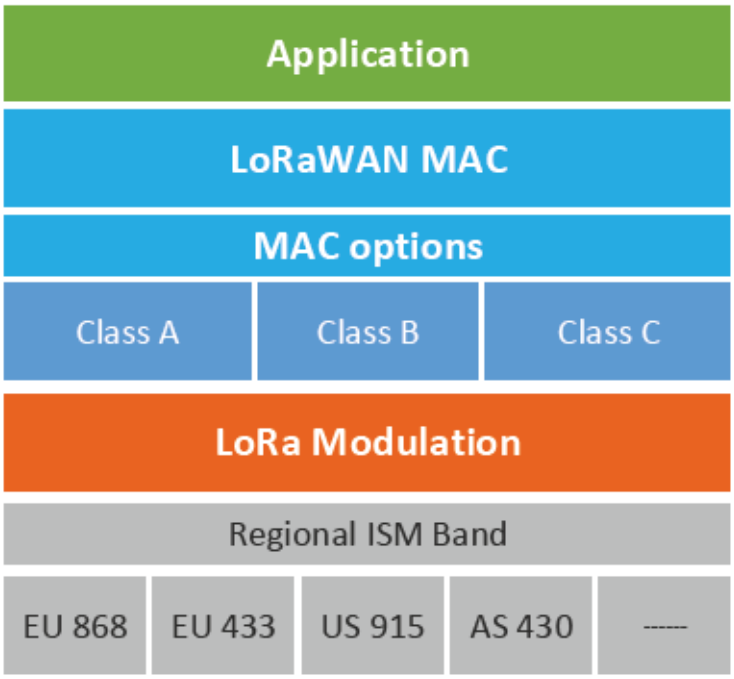

Figure 11. LoRaWAN protocol stack.

Extensive measurement campaigns show that the communication range of LoRa reaches up to 30 km over the water and more than 15 km on the ground [42]. LoRa is suitable for a wide range of telemetry applications (e.g., sensing and monitoring), which can be used in several industry verticals, such as smart grids and cities, and smart agriculture up to industrial IoT applications. During the past few years, many studies have contributed by proposing new algorithms, systems models, analyses, and by designing new approaches for performance enhancement of LoRa networks.

3.1 LoRa PHY

LoRa provides good performance in terms of reliability and energy consumption. It operates at unlicensed frequency ISM (Industrial, Scientific, Medical) bands of 863-870 MHz and 915 MHz in Europe and the U.S., respectively [50, 51]. In Europe, the duty cycle

limitations range from 0.1% to 10%, following European Telecommunications Standards Institute (ETSI) standards. In addition, LoRa works on variable and adaptive data rates by using different spreading factors. This is achieved by the NS controlling the spreading factors (SFs) and bandwidth (BW) of the end-devices. Higher SFs allow higher communication links; however, as a drawback, they reduce the data rate and increase the time-on-air (ToA) of LoRa packets [52].

Considering the $BW = 125$ kHz, every LoRa packet is prepended with a preamble to authorize it for the timing and frequency synchronization at the receiver side, 0.3 kbps to 11 kbps is the limitations for the actual data rate. Overall, the capacity of the system is higher because the receiver has ability to simultaneously receive the transmissions from the various nodes by exploiting the orthogonality of SFs that are used by LoRa. The LoRa modulation bit rate is defined as [53]

$$R_b = \frac{4}{4+CR}\frac{BW}{2^{SF}}, \tag{1}$$

where $\frac{4}{4+CR}$ is the effective coding rate, ranging from $\frac{4}{5}$ to $\frac{4}{8}$, while CR denotes the LoRa coding rate configuration, varying from 1 to 4. For instance, Table 4 shows the characteristics of 9 byte LoRa packets with explicit header and CRC modes enabled and $BW = 125$ kHz.

Table 4. Characteristics of the LoRa uplink model containing packets of 9 bytes at BW = 125 kHz, where l_i, l_{i+1} are inner and outer radii of i-th annulus representing specific SF.

SF (i)	Bit Rate kbps (Rb_i)	Receiver sensitivity dBm	SNR dB (q_{SF})	Range km
7	5.47	-123	-6	$l_0 - l_1$
8	3.13	-126	-9	$l_1 - l_2$
9	1.76	-129	-12	$l_2 - l_3$
10	0.98	-132	-15	$l_3 - l_4$
11	0.54	-134.5	-17.5	$l_4 - l_5$
12	0.29	-137	-20	$> l_5$

Figure 12 demonstrates the physical layer message format. The physical layer header (PHDR) is 16 bits long and physical header cyclic redundancy check (PHDR_CRC) has 4 bites. Moreover, uplink communication further uses 16 bits for CRC to detect the transmission errors. A LoRa packet can carry a maximum payload of 255 bytes.

Figure 12. Message structure of LoRaWAN physical layer.

In message format, preamble is responsible for the synchronization of the receiver with the incoming data follow. There are two options for the header, in explicit mode

operations the header defines the length of payload, forward error correction (FEC) code rate and availability of CRC in the frame. On the other hand, in an implicit mode, the payload and code rate are fixed that don't contain any field to define the parameters which reduce the transmission time. The ToA of a LoRa packet depends on given value of SF, BW and CR. The mathematical relation between symbol period and symbol rate is given as [54]

$$T_S = \frac{1}{R_S}, \tag{2}$$

$$R_S = \frac{BW}{2^{SF}}, \tag{3}$$

The LoRa packet duration depends on the the sum of duration of the preamble and sent packet. Preamble length is express as

$$T_{preamble} = (n_{preamble} + 4.25)T_S, \tag{4}$$

where $n_{preamble}$ is the length of programmed preamble. The length of payload symbols is defined as [55]

$$n_{payload} = 8 + max(ceil[\frac{8PL - 4SF + 28 + 16CRC - 20IH}{4(SF - 2DE)}](CR + 4), 0), \tag{5}$$

where CR is code rate ranging from 1 to 4, DE represents the low data rate optimization and it can be enable by setting $DE = 1$, where $IH =$ is set to 1 when there is no header and it is 0 when header mode is enabled. PL denotes the size of payload in bytes, and SF is representing LoRa Spreading Factor.
The payload duration is product of number of payload symbols and symbol period, which is given by

$$T_{payload} = n_{payload} \times T_S, \tag{6}$$

It is worth noting that the payload duration depends on the chosen header mode. The ToA of LoRa packet is sum of playload and preamble duration express as

$$T_{OA} = T_{preamble} + T_{payload}, \tag{7}$$

From the above equations, it is clear that the SF and size of payload have a direct impact of the ToA of LoRa packets. The ToA also varies by changing the value of the code rate. BW also has an influence on the ToA of LoRa packets, higher BW leads to lower ToA.

3.2 LoRa MAC

The LoRa protocol stack with a MAC defined by LoRa Alliance is known as LoRaWAN [56], it is a type of ALOHA protocol controlled by the NS. In LoRaWAN, the adaptive data rate enables the NS to adjust the transmission rate of a node by

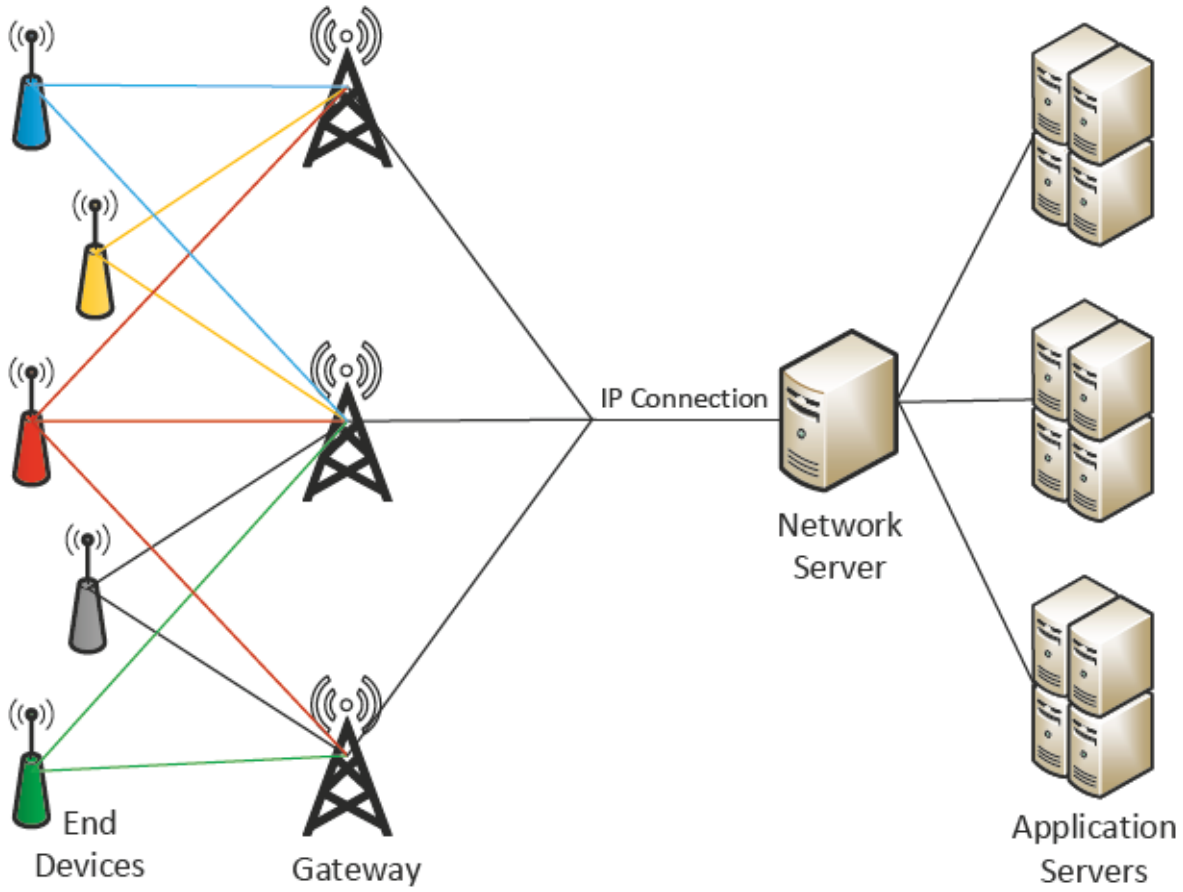

Figure 13. LoRaWAN network architecture.

changing the SF selection, a suitable trade-off between the communication link robustness and energy efficiency. The network architecture contains end-devices, gateways, and a NS, forming a star topology. Figure 13 shows the network architecture of LoRaWAN containing sensors node, gateway, NS, application server, and users.

Notably, the gateways has the ability to receive data from multiple nodes at the same time because of the orthogonality of sub-bands and the quasi-orthogonality of different SFs. LoRaWAN defines three classes of devices depending upon the application. End-devices transmit the LoRa packets to the gateway using the different SFs. It also has ability to receives the traffic through downlink. Gateway receives packets from the LoRa end-devices and transmit the data packets to the NS through an IP connection for further processing. NS is considered as a controller of the network and central coordinator. It is responsible for parameters adaptation and decision making. After the specific operation, it forwards the packets to the application server. Figure 14 illustrates the protocol architecture of the LoRaWAN.

LoRaWAN promises end-to-end encryption and data integrity. Application Session Key is used to provide confidentiality in the upper layer payloads. Conversely, Network Session Key provides data integrity on the top of ciphertext payload and a subset of header portions. Energy efficiency is achieved through an ALOHA channel access approach. When a node wants to transmit a packet, it does not execute any previous inspection of

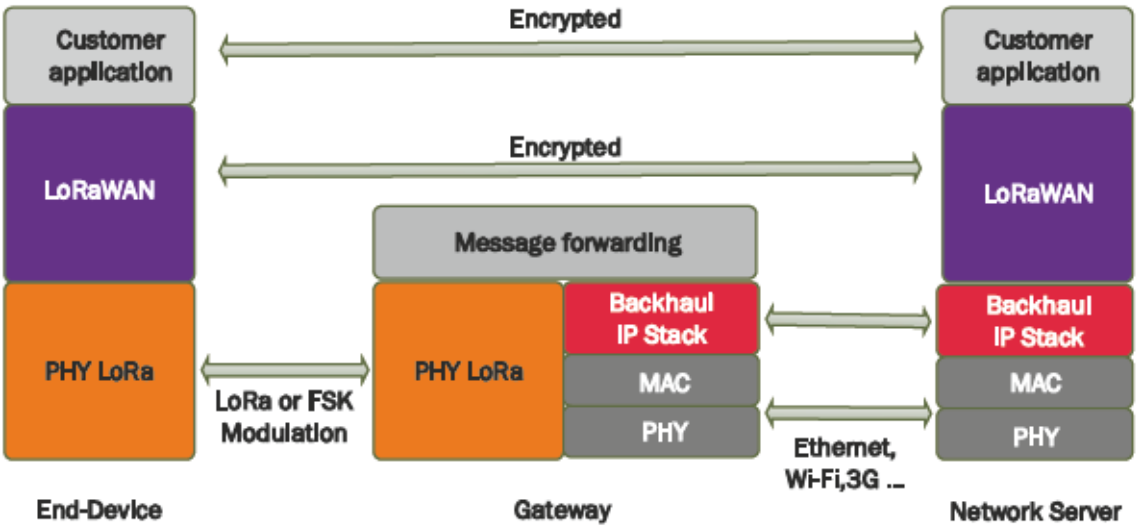

Figure 14. LoRaWAN protocol structure.

the channel for avoiding collisions possibilities. The message structure of LoRa MAC is illustrated in Figure 15.

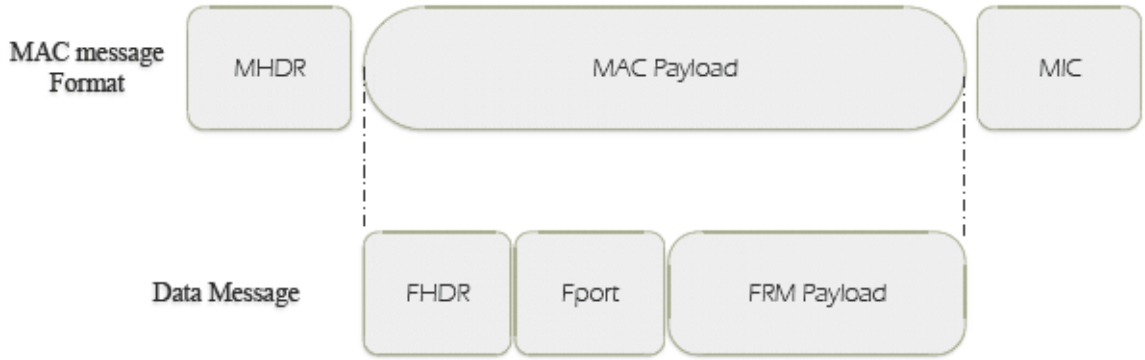

Figure 15. Message structure of LoRa MAC.

It comprises MAC header known as MHDR that is used to define the type of MAC message. The MAC payload contains a join message and application data. At the receiver side, the integrity of the received MAC message is checked by the Message Integrity Code (MIC) which is 4 bytes long. Data messages can accommodate MAC commands in frame payload (FRM Payload), it can also transfer through the frame header (FHDR) relying on the value of Fport (1 byte). The FHDR has the length of 7 bytes to 22 bytes. MAC commands are used for the configuration of MAC layer and radio parameters [57].

Depending on the different requirements of application scenarios, LoRaWAN defines three classes of sensors. LoRaWAN Class A user nodes have three type of transactions including unconfirmed uplink transmission (without ACK), confirmed uplink mode (with ACK), and uplink-downlink operation mode that has reply data functionality from the

Application Server. In confirmed uplink mode, Class A devices wait for ACK only in their receiving windows (RX1 and RX2) and consume the least power. After every uplink transmission, a device opens RX1 and RX2 windows for listening response from NS. These windows are activated after RECEIVE_DELAY1 and RECEIVE_DELAY2, respectively. For the next transmission, device cannot transmit and it has to wait for ACK in receiving windows. If there is no response from the NS within the specific period then device may retransmit the preceding packet. RX1 and RX2 are mainly defined on the basis of data rate and offset time (ACK timeout). The configuration of offset time of RX1 and RX2 is possible through MAC commands or assign 1 second and 2 seconds, respectively. For the downlink transmission, Class A device gets data by sending unconfirmed message. Downlink data is received in RX1 when the RX2 is disabled.

Class B devices are able to open extra receiving windows at scheduled times, thus reducing downlink latency. It enables the NS to know when the node is listening. The devices are expected to get Beacon_Period from the gateways and wakes up at every Beacon_Period to synchronize with gateways to active the receive windows. Class B devices allows the gateway to send any command from NS to sensor node within a Beacon_Period.

Finally, Class C nodes consume the most energy because they leave the receiver enabled all the time, allowing for the lowest latency time. Instead of waiting for RECEIVE_DELAY1 before receptions, in Class C devices the ACK messages can be received immediately. In the IoT domain, LoRaWAN is appears as a holy grail because it has the ability to resolve many challenges such as providing massive connectivity for large-scale application scenarios, and ensuring the low energy consumption. Figure 16 shows the overview of LoRaWAN classes transmissions.

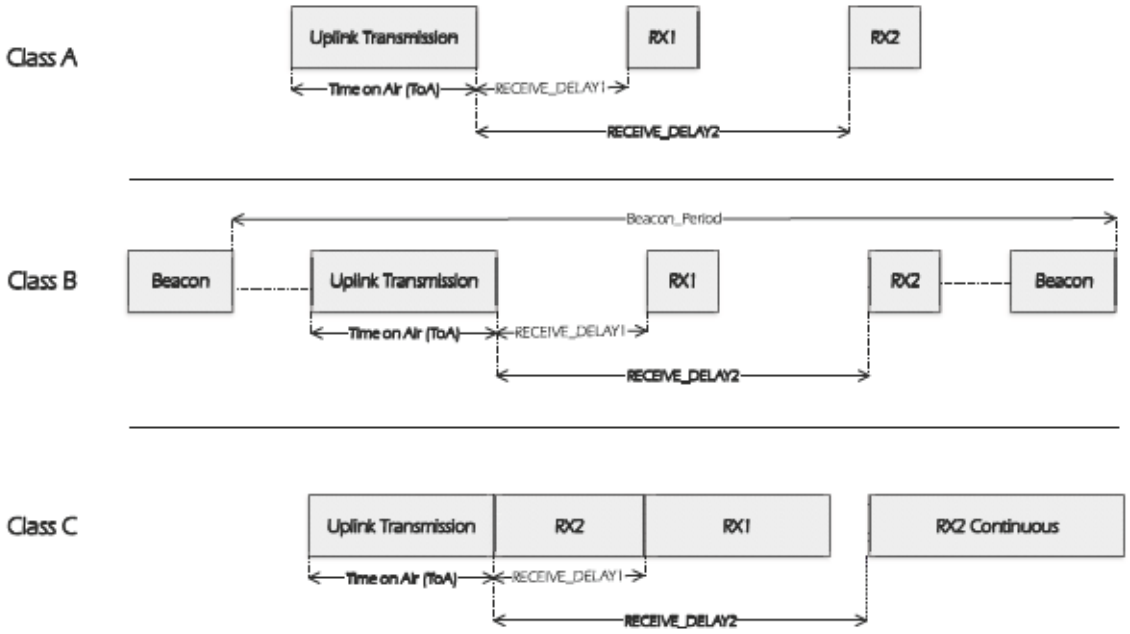

Figure 16. The operations of LoRaWAN devices' classes.

4 SMART CAMPUS MTC TRAFFIC CHARACTERIZATION: 5GTN LORA USE-CASE

In this chapter, we present the overview of IoT services integration with 5G and LoRaWAN based digital campus. The primary aim of 5G wireless technology is to attain three major requirements including ultra-reliable low latency communication (URLLC), enhanced mobile broadband (eMBB) and massive machine-type communication (mMTC). The URLLC is responsible for low latency transmission with large reliability through a small set of terminals. While eMBB establishes a stable connection that can support very high peak data rates and also handle data rates for the cell-edge users. The mMTC supports numerous IoT devices. Network slicing of Radio Access Network (RAN) through orthogonal resource allocation is used to achieve these services [58]. The rapid growth of IoT applications request mMTC to support massive connectivity with low-power consumption and suitable reliability. LPWAN technologies handles the first two requirements of mMTC. However, to attain the target of massive IoT devices connectivity and energy-efficiency, LPWANs overcome the drawbacks of complex channel control mechanisms by replacing them with straightforward MAC protocols, with the sacrifice of reliability [59].

4.1 5GTN at The Univesity of Oulu

World's widest 5G Test Network (5GTN) with open access is deployed in Oulu, Finland that provides the special unique options for testing of 5G applications, services and technologies in real time. The University of Oulu and VTT Technical Research Centre of Finland provides the required essential for the 5G testing and trials. Wireless access IoT (LoRa, NB-IoT, LTE-M1) of 5GTN provides access to the IoT network that enables the testing of application and provides an actual environment for research and development. It has operational functionalities of SDN and NFV. Furthermore, the 5GTN contains many sites and is linked with local and international testing environments. It supports the use of 5G smart devices, multiple frequency bands and testing systems. 5GTN is an evolution of LTE to 5G radio access, that integrates Wi-Fi and IoT networks, provides cloud systems for applications, it brings services close to the users through the Multi-access Edge Computing and also provides secured network connections to the other 5G networks across the world [60]. The network architecture and integration of IoT sensors with 5GTN is illustrated in Figure 17.

4.2 Smart campus

An end-to-end IoT environment with large and dense sensors is deployed inside 2163.8 square meter area of Tellus Innovation Arena, University of Oulu, Finland for the purpose of building digital campus. The sensors acquire the information of CO_2, humidity, person mobility through passive infrared (PIR), temperature and light. There are 331 ($ELSYS$ ERS CO_2) LoRaWAN devices through the area of Tellus. These devices contain light, temperature, humidity, air quality and infrared motion sensors. They are simple to

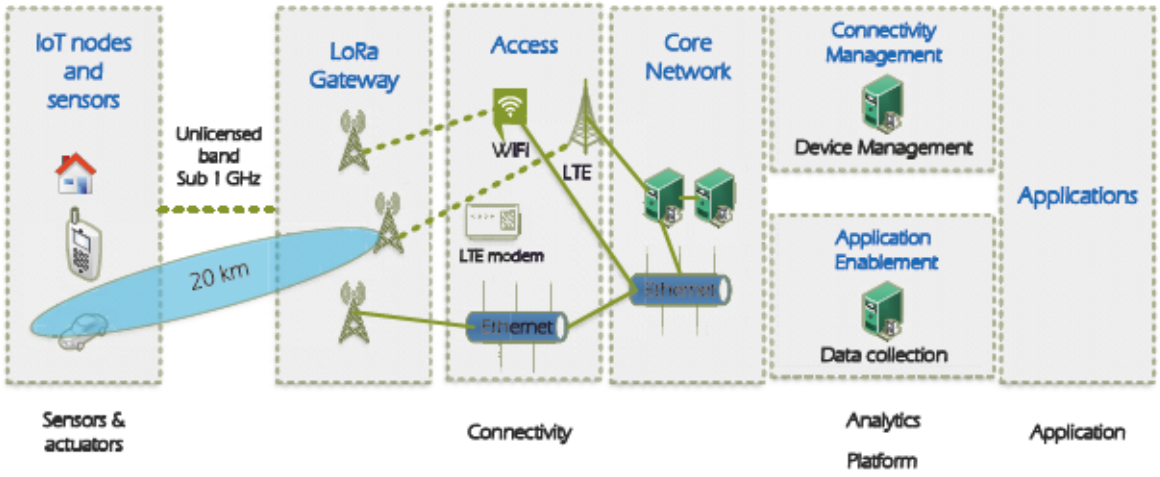

Figure 17. IoT nodes and sensors integration with 5GTN.

configure, which enables easy test setups. Sensor's battery lasts up to 10 years and it is powered by two AA lithium batteries of 3.6V [61].

Authors in [27], calculated the total number of required sensors for deployment inside the target area. For the seek of better coverage, they placed the gateway at a suitable location. Finally, they tested the signal's quality for different DR. In deployed LoRa network, each packet has a fixed length, transmissions are through SF7 using transmit power of 14 dBm in absence of downlink channel, nodes are initializing at a random time. A collision takes account whenever two or more nodes transmit using the same SF and frequency channel. Figure 18 presents the 5GTN LoRaWAN network architecture.

Network deployment contains Multitech Conduit gateway that has ability to operate over a 4G and 5G cellular backhaul. They placed the gateway antenna at the height of 24 meters, 180 meters away from the targeted area (Tellus) for the better coverage. The sensor nodes transmits the packets to the gateway through three LoRaWAN channels (868.10 MHz, 868.30 MHz, and 868.50 MHz). The sensor nodes are authenticated with the gateway by using OTAA that requires a globally end device identifier, application identifier, and AES-128 key. Node-RED handles and visualizes the received LoRaWAN packets. It also allows the communication between the gateway and ThingWorx. For that purpose, they deployed an application on the top of the gateway to forward the acquired sensor data to ThingWorx IoT platform that stock the data over the MQTT protocol. Multiple users can subscribe and post messages to broker on the top of the Transmission Control Protocol/Internet Protocol. The ThingWorx is client of MQTT, that is linked with MQTT broker and approves message transmission between LoRaWAN and ThingWorx.

Furthermore, the stored data from ThingWorx can be access through application program interface (APIs) based on HTTP. The application layer handles the management and analysis of acquired sensor data. To achieve this goal, it contains different components, first part uses an automated Python script that receives new data messages from the ThingWorx and saves it in a database (PostgreQSL). In addition, it also stores the location details of every individual sensor [62, 63].

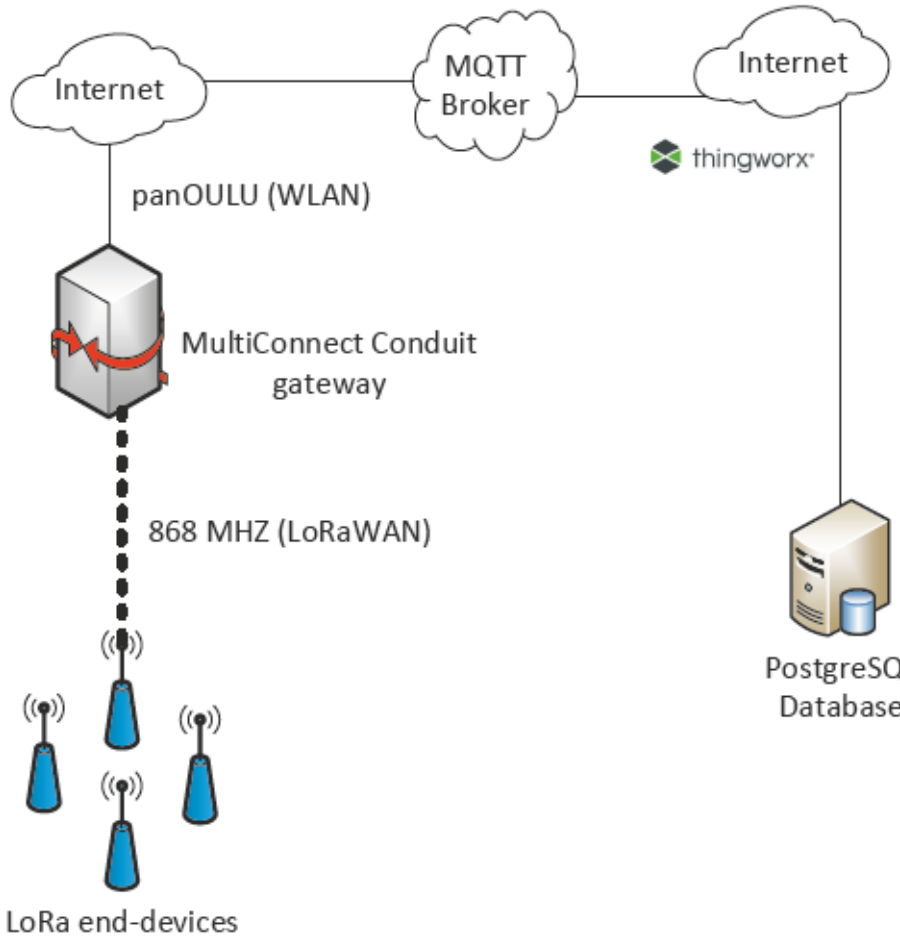

Figure 18. Network architecture of 5GTN LoRaWAN.

In the context to understand the traffic characteristics of 5GTN LoRaWAN, We analyse the sensor data and observe that humidity, temperature and CO_2 measurements do not change dramatically. The transmission of LoRa packets are scheduled every 15 minutes.

4.3 5GTN LoRa Traffic Characterization and Modeling

In this subsection, we perform analyses for the statistical behaviour examination of 5GTN LoRaWAN traffic and model the aggregated traffic arriving at the gateway. 5GTN LoRa network aggregated traffic modeling is focus of this thesis work, for which we provide a relatively simple traffic aggregation model for the LoRa gateway. Mostly, the IoT traffic is more dominated by uplink as compared to the conventional cellular networks and normally nodes are sending data on a regular basis with small payloads. Sometimes, multiple end-devices can transmit the packets within a small interval of time, exhibiting spatial and high temporal correlation. For instance, a smart meter

sends hourly updates to the network server. Source level mathematical models are the representation of device level IoT traffic, and because of a demanding source by source characterization, it can be complex for larger simulations. Conversely, aggregated traffic models are simpler as compared to source traffic models but it just models the network traffic at the gateway [28].

5GTN LoRaWAN data set is used for the analysis of the traffic. In June 2018, 331 devices were transmitting their packets. Each device ideally transmits 96 packets per day, and each individual device is transmitting after the interval of 900 seconds.The node selects one of the three communication channels randomly to transmit a packet. The details of channels are mentioned below:

331 LoRa devices transmits = 331 × 96 = 31776 packets per day.
Channel 0: 868.10 MHz
Channel 1: 868.30 MHz
Channel 2: 868.50 MHz
One Single Channel transmits = 31776/3 = 10592 packets daily

On the experimental period, Channel 0 (868.10 MHz) and Channel 2 (868.50 MHz) performed efficiently but Channel 1 (868.30 MHz) experienced a large number of packet losses. Figure 19 demonstrates the number of received packets from all devices in an interval of 15 minutes for June 4, 2018 for all the channels, and the same statics for individual channels.

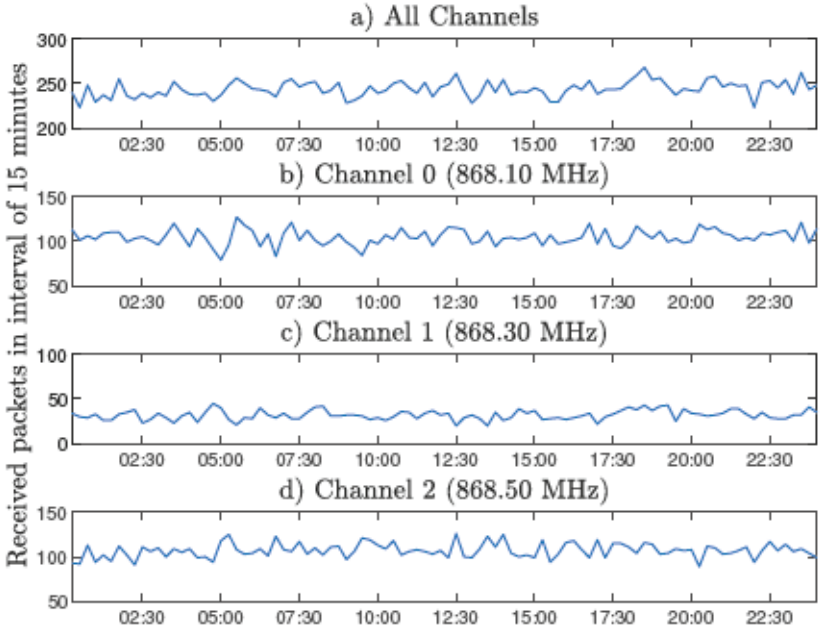

Figure 19. Number of received packets from all LoRaWAN nodes in interval of 15 minutes through communication channels 868.10 MHz, 868.30 MHz and 868.50 MHz for June 4, 2018.

As illustrated in Figure 19, we can observe that Channel 1 received lesser packets as compared to other two channels. In our analysis, we excluded the packets of Channel 1 (868.30 MHz) for better modeling of the aggregated traffic. The rest of two channels 868.10 MHz and 868.50 MHz have almost the same behaviour and very low PER (approximately 4%). To analyse the daily traffic behavior, we conducted the measurements that shows received packets from all of the LoRa devices in 15 minutes interval for different Mondays (June 4, June 11, June 18 and June 25) of the month June, 2018. For the selected days, the total number of received packets are almost close to each other: 23403, 23610, 23645 and 23514, respectively. Nodes transmit through the three communication channels: 868.10 MHz, 868.30 MHz and 868.50 MHz. As previously discussed, Channel 1 has a huge packet error rate (PER), that is why we excluded its packets. For the said dates, the number of packets received through Channel 0 (868.10 MHz) and Channel 2 (868.50 MHz) are 20327, 20548, 20580, and 20415 for June 4, June 11, June 18 and June 25, respectively, as depicted in Figure 20 and Table 5 .

Table 5. Number of transmission for different Mondays of the June, 2018.

Channels	June 4	June 11	June 18	June 25
Channel 0	10044	10174	10346	10218
Channel 1	3076	3064	3065	3099
Channel 2	10283	10374	10234	10197
Total	23403	23610	23645	23514
PER	26.35%	25.70%	25.59%	26%

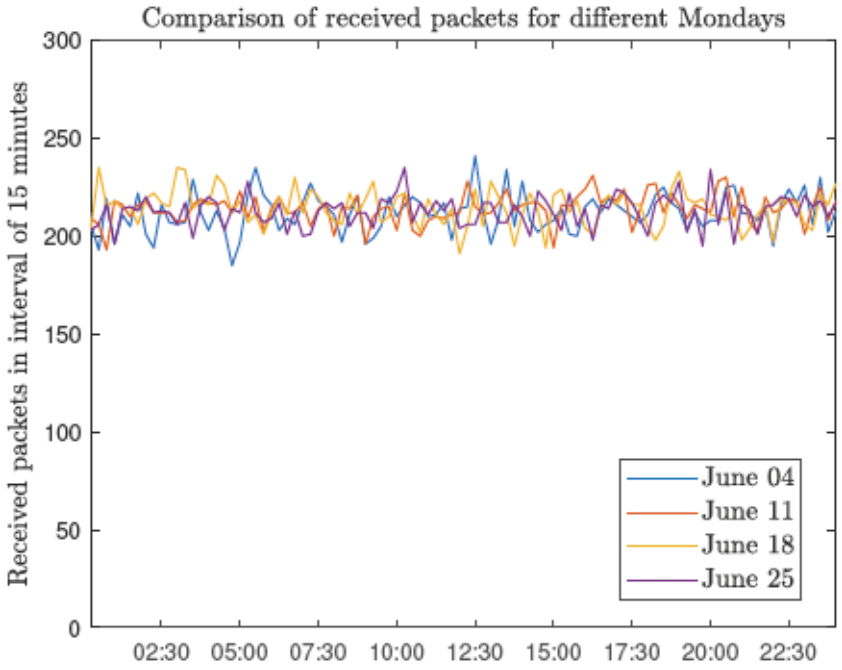

Figure 20. Comparison of received packets from all nodes in interval of 15 minutes from all the sensors node for the different Mondays of the June,2018.

4.3.1 Inter-arrival time and Data fitting

To perform an in-depth analysis of traffic behavior, we calculate the inter-arrival times of the traffic arriving at the gateway. Our work uses gateway timestamp for comprehensive and thorough inspections of inter-arrival times. By definition, inter-arrival time is the time difference between the arrival of two consecutive packets at the system. The arrival rate is the number of packets that arrives in per unit of time. The relation between arrival rate and mean inter-arrival time can be expressed as $\mu = \frac{1}{\lambda}$, where λ is the arrival rate and μ is average inter-arrival time.

To deeply understand the patterns of 5GTN LoRaWAN traffic, we measure the inter-arrival times of received packets for different weeks: June 1 - June 7, June 8 - June 14, June 15 - June 21, and June 22 - June 29 of 2018. For the said period, the total number of received packets are almost close to each other: 142974, 143747, 143774 and 143300, respectively. From the probabilistic point of view, the normalized histogram of inter-arrival times demonstrate exponential behavior for all the selected data set. The exponential distribution is suitable for modeling the pattern of waiting times, in a scenario when the possibility of waiting an extra period is not dependent on how much time you have waited already. The mathematical expression of exponential probability density function can be defined as

$$f\big(x;\lambda\big) = \begin{cases} \lambda e^{-\lambda x} & x \geq 0 \\ 0 & x < 0 \end{cases} \tag{8}$$

where x represents the amount of time between the arrival of packets. After the analytical examination, we fit the inter-arrival times into the exponential distribution using maximum likelihood estimation (MLE) to measure the average inter-arrival time (μ) for the specific chosen period. Let us consider a data set consists of n packets arrivals. The inter-arrival between packets arrivals is denoted as $x_i = t_{i+1} - t_i$ for $(i = 1, \ldots, n-1)$. The likelihood function for the arrival rate is given as

$$MLE(\ \lambda | x_1, x_2, \ldots, x_{n-1}) = \lambda^{n-1}[e^{-\lambda(x_1+x_2+\cdots+x_{n-1})}], \tag{9}$$

To find the maximum likelihood, we derivative the (9) and solve for λ when the deivative is set to be equal to 0 for finding the optimal value.

$$\frac{\partial}{\partial\lambda}\lambda^{n-1}[e^{-\lambda(x_1+x_2+\cdots+x_{n-1})}] = \frac{\partial}{\partial\lambda}\big(n-1\big)\log\big(\lambda\big) - \lambda\big(x_1 + x_2, \cdots + x_{n-1}\big), \tag{10}$$

$$0 = \big(n-1\big)\frac{1}{\lambda} - \big(x_1 + x_2 + \cdots + x_{n-1}\big), \tag{11}$$

when we further solve (11), it gives the maximum likelihood estimation for $\lambda = \frac{n-1}{\big(x_1+x_2+\cdots+x_{n-1}\big)}$ and it's reciprocal is mean inter-arrival time (μ). As a part of traffic modeling, μ is used to generate the exponential probability density function that shows the aggregated traffic model of 5GTN LoRa network.

Figure 21 depicts the normalized packet arrival probability of actual and analytical aggregated traffic as a function of inter-arrival times. It is possible to see that the majority of traffic arrives within a 10 seconds interval. Conversely, just a few of the packets have inter-arrival time of 20 seconds or higher. This is probably due to the periodic nature of the traffic, as mentioned in Subsection 4.3, 5GTN LoRaWAN nodes are configured to transmit with the interval of 15 minutes.

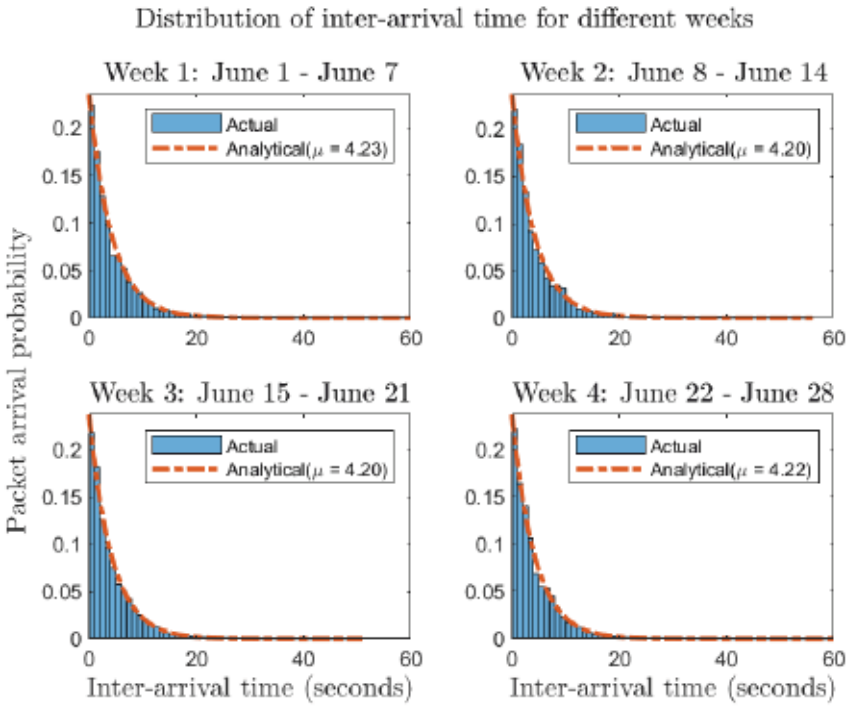

Figure 21. Normalized probability distribution of LoRa packets as function of inter-arrival times for four weeks of June, 2018.

With the motivation to further inspect the traffic characteristics for days, we select the busiest day and the least busiest day also named lightest day from the data set. Busiest day received in total 20674 packets transmitted over the Channel 0 and Channel 2. On the other hand, the lightest day received 20211 packets received by the same channels. Furthermore, it is concluded from the statistical examination that the distribution of traffic arrival was exponential. Same as the weekly patterns, most of the traffic arrives within 10 seconds interval while only few packets had inter-arrival time of over 20 seconds. Figure 22 shows the statistical pattern of traffic for busiest and lightest day of June, 2018. Similarly, we decide to further narrow down our analysis to inspect the traffic characteristics for the different hours: 00:00-01:00, 06:00 - 07:00, 12:00 - 13:00, and 18:00 - 19:00 of a day (June 1, 2018). As expected, the statistic behavior followed a similar pattern as like previous two scenarios. It is also worth noting that most of the received packets have inter-arrival times lower 10 seconds and only a few exceeds 15 seconds. This way, we can see that the traffic patterns are consistent for different weeks, days and hours. In essence, this means that the average inter-arrival time remains almost constant, with a slight change between 4.1 to 4.2 seconds. Figure 23 demonstrates the normalized packet arrival probability of actual and analytical aggregated traffic as a function of inter-arrival times for different hours of June 1, 2018.

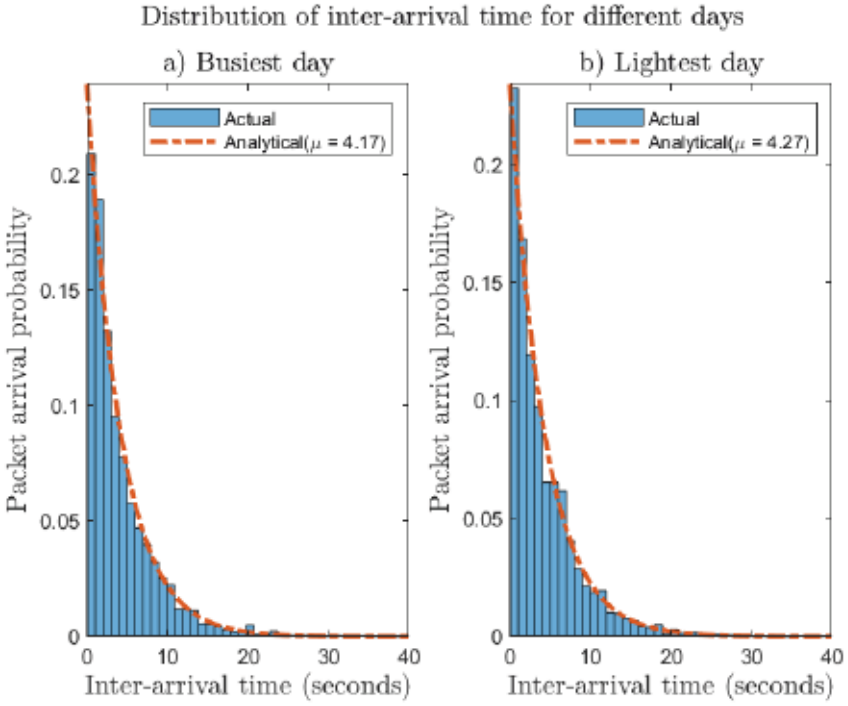

Figure 22. Exponential probability density function of inter-arrival times for busiest and lightest day of June, 2018.

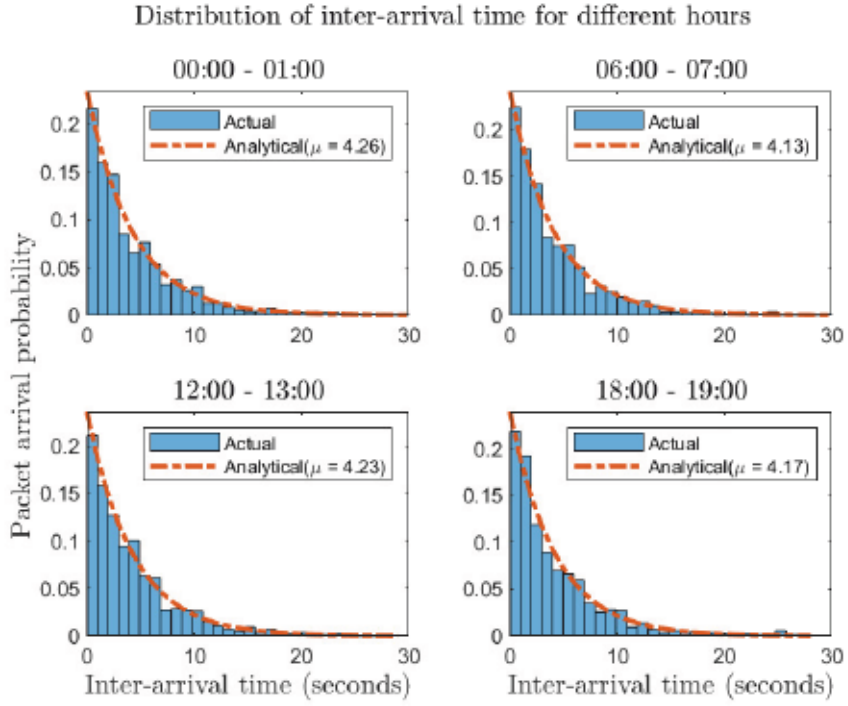

Figure 23. Exponential probability density function of inter-arrival times for different hours of a day (June 1, 2018).

As discussed in Subsection 4.3, theoretically every single device ED_j for $(j = 1, \ldots, 331)$ is a traffic source which starts transmitting it's first packet at time $R_j \sim$

$U(0, I)$. After that, it periodically transmits at $R_j + KI$ for $K = 0, \ldots, 95$, where $I = 900$ seconds is constant report period of sensor nodes. With motivation to study the theoretical model, we generate aggregated traffic (assuming no packet losses) of 331 devices for one day and compare it with the characteristics of actual aggregated traffic of 5GTN LoRaWAN. The statistical results reveal that inter-arrival times of both theoretical and experimental models have exponential distributions but different mean inter-arrival times (μ). Figure 24 illustrates the comparison of experimental and theoretical traffic models.

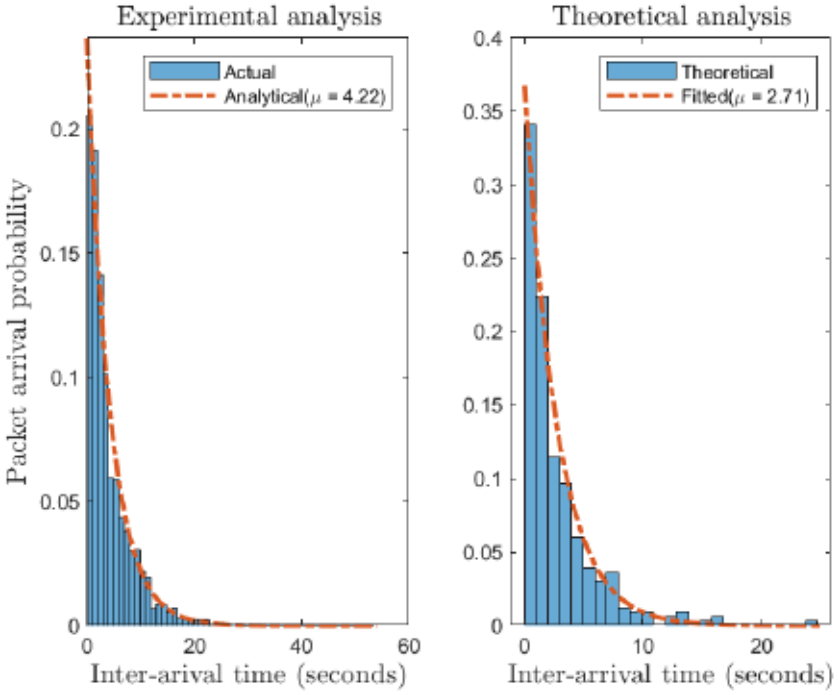

Figure 24. Comparison of experimental (June 7, 2018) and theoretical traffic models.

The difference in analytical and theoretical mean inter-arrival times motivate us to verify the analytical traffic model, thus we compare the average inter-arrival time of modeled traffic with the actual 5GTN LoRaWAN data set. From the actual 5GTN data set, we calculated average delay for the different number of aggregated packets $N_P = 1$, 10, 30, and 60 to compare it with the analytical delay. The mathematical expression to calculate the average measured delay for a given N_P is expressed as

$$\overline{D}_{N_P} = \frac{1}{T} \sum_{j=1}^{T} \triangle D_j \ \forall j \in 1 \ldots T, \tag{12}$$

where $\triangle D_j$ is the delay of a aggregated packet. For instance, the measured delay for $N_P = 60$ is equal to the time $\triangle D$ that transmissions 60 LoRa packets take from first transmission to the 60^{th} transmission. Figure 25 illustrates the graphical representation of the measured delay for $\overline{D}_{60}$.

In communication networks, we can find the times for how long a packet will wait in a queue and how much time that packets wait through the queuing theory. In queueing theory, the poisson process is widely used with the arrival rate of λ customers per second. The probability of N_P arrivals in an interval of S time is defined as

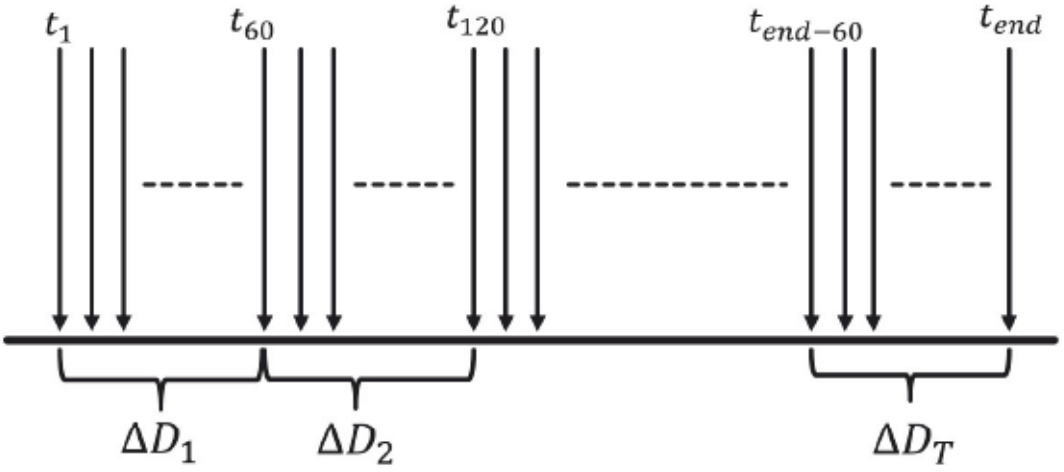

Figure 25. Representation of the packets arrivals and delay calculated for $\overline{D}_{60}$, where t_1 and the t_{end} are the time of first and last arrival in the data set, respectively.

$$P(N_P) = \frac{(\lambda S)^{N_P} e^{-\lambda S}}{N_P!}, \tag{13}$$

We considered single server queues (M/M/1) and the queueing model is illustrated in Figure 26.

Figure 26. The architecture of the queueing model.

According to Little's law, the average number of packets in a system is equal to the product of the average arrival rate (λ) and the waiting time (W) defined as

$$L = W \times \lambda, \tag{14}$$

Hence, the waiting time that a packet spends from entering system until completion of the service is given by

$$W = \frac{L}{\lambda} = \frac{\rho}{\lambda(1-\rho)} = \frac{1}{S_R - \lambda}, \tag{15}$$

Similarly, the waiting time that a packet spends in queue is expressed as

$$W_q = \frac{L_q}{\lambda} = \frac{\rho^2}{\lambda(1-\rho)} = \frac{\rho}{S_R - \lambda}, \tag{16}$$

where L is size of system which defines the expected number of packets in the system and L_q is size of queue, where ρ is utilization rate which is defined as $\rho = \frac{\lambda}{S_R}$, and S_R denotes service rate.

We calculated the actual average delay from the 5GTN LoRaWAN data set. Queuing theory is used to estimate the analytical delay for a different number of aggregated LoRa packets N_P = 1, 10, 30, and 60. We compare the measured delay (calculated data set delay) with the analytical delay and conclude that that data and analytical analysis are matching. On the other hand, theoretical results differs from the experimental mean inter-arrival times. Table 6 shows average waiting delays for different aggregated packets.

Table 6. Average waiting delays for different number of packets.

Delays	$\overline{D}_1$	$\overline{D}_{10}$	$\overline{D}_{30}$	$\overline{D}_{60}$
Measured Delay	4.21	42.17	126.53	253.06
Analytical Delay	4.2	42	126	252
Theoretical Delay	2.71	27.1	81.3	162.6

To understand this gap in experimental and theoretical results, we dive into the data set to carry out further study about the individual sensor in terms of successfully received packets at gateway. We examine the performance of all 331 sensors for the consideration period of a month. The concluded results are demonstrated in Figure 27, it is clear that node *a8-17-58-ff-fe-03-0f-51* has performed almost same as ideal case with 1% PER. Conversely, nodes *a8-17-58-ff-fe-03-0f-9d* and *a8-17-58-ff-fe-03-0f-d6* showed lowest (34.79% PER) and moderate (16.52 % PER) outcome, respectively - in terms of successful delivery of packets. Possibly, the variations in PER of sensors could be one of the reason behind unlikelihood of experimental and theoretical mean inter-arrival times. Due to the fact that network impairment can impact the characteristics of the traffic, hence optimization and modeling of traffic solely based on theoretical estimation is not a practical and right choice.

4.4 5GTN LoRa Traffic aggregation

In this subsection, we examine the network goodput as a function of the number of aggregated LoRa packets to optimize the typical LoRaWAN packet forwarding protocol. Goodput is the application level throughput of communication networks. It is the amount of useful data bits delivered by the communication network to the specific destination per unit of the time [60]. The number of information excludes the overhead bits of protocol and the re-transmissions. It links this to the duration from the transmission of first bit of the first packet until it transmits all the bits of final packet. For instance, if a data file is delivered, the goodput would be equal to the number of useful information bits transmitted divided by the transmission time of a file. The goodput of the system is always less than its throughput. There are three factors behind it: protocol overhead, re-transmissions and flow control and congestion avoidance of the transport layer. Normally, the network, transport, and datalink layer protocol's overhead is included in throughput, but not for goodput.

For instance, transmission control protocol (TCP) slow start can cause a drop in the goodput. Re-transmission of the packets because of automatic repeat request (ARQ) due

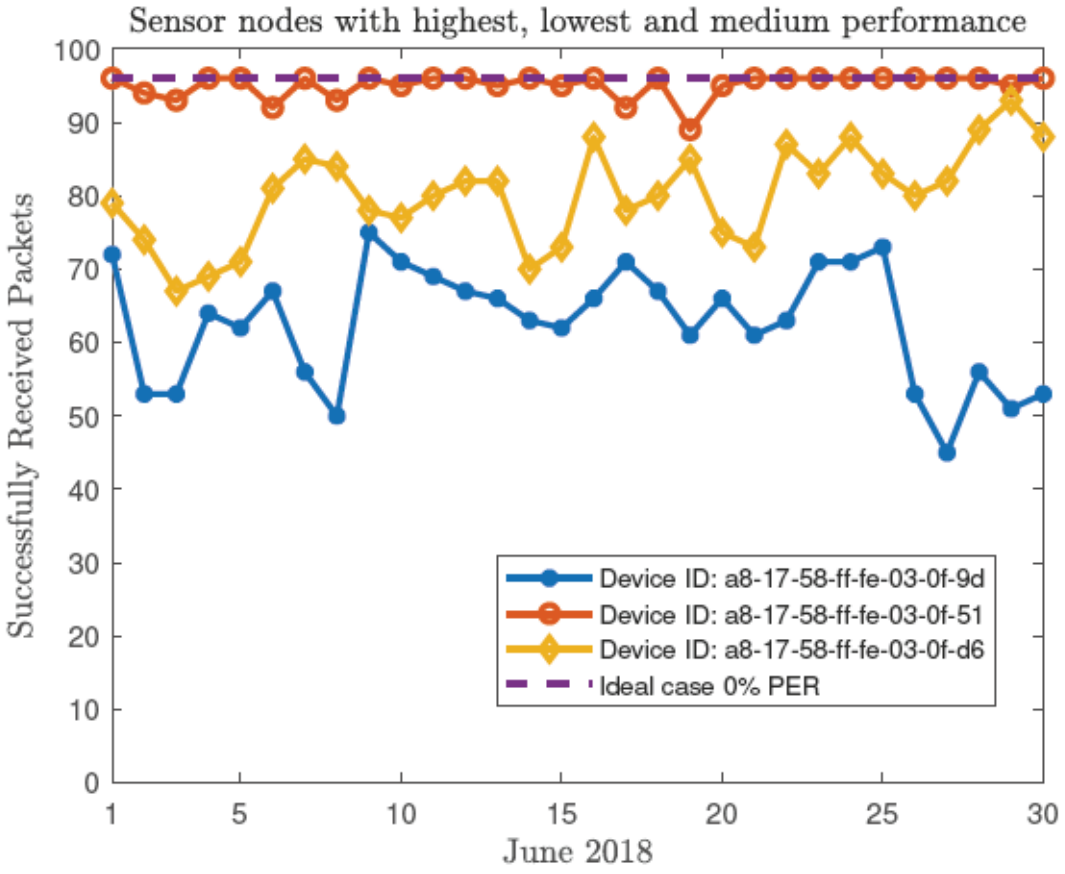

Figure 27. 5GTN LoRaWAN sensor nodes with highest, medium and lowest performance for June, 2018.

to packet dropping also lowers the goodput. Assume that it forward a data file using HTTP through a switched Ethernet with total a channel capacity of 100 megabits/s. The system cannot transmit the file directly as a one continuous data stream. Rather than it, the file must be broken down in small chunks of data. Figure 28 demonstrates the Ethernet frame structure.

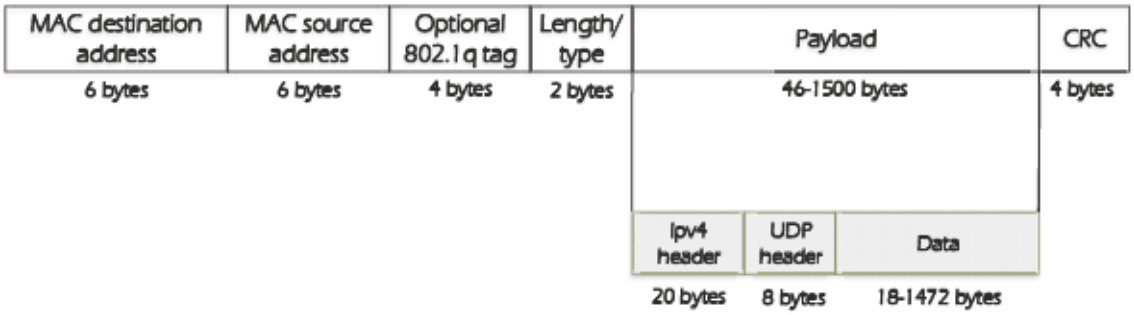

Figure 28. Ethernet packet format with description of payload bytes.

The individual chunk size should not be more than maximum transmission unit of IP over Ethernet that is 1500 bytes. TCP and IPv4 header uses 20 bytes each, with results

in a useful 1460 bytes per packet. Since the Ethernet protocol has 22 bytes of overhead, we have a packet with a maximum total length of 1522 bytes. Moreover, the maximum goodput ratio of the system is equal to 1460/1522. Finally, the maximum goodput results by multiplying the channel capacity and the maximum protocol goodput ratio.

In related work [27], 331 LoRa devices send packets to the gateway with a mean inter-arrival time of 4.2 seconds. As discussed in Subsection 1.4, a typical LoRa gateway forwards one packet at a time [39] to NS, which respond to each transmission with an acknowledgement message. As a consequence, it can cause heavy traffic problems for a large-dense deployment scenario. In addition, this traditional gateway to the server interface consumes more resources and power because of individual transmissions. Figure 29 depicts the typical upstream LoRa gateway message forwarding protocol without packet aggregation.

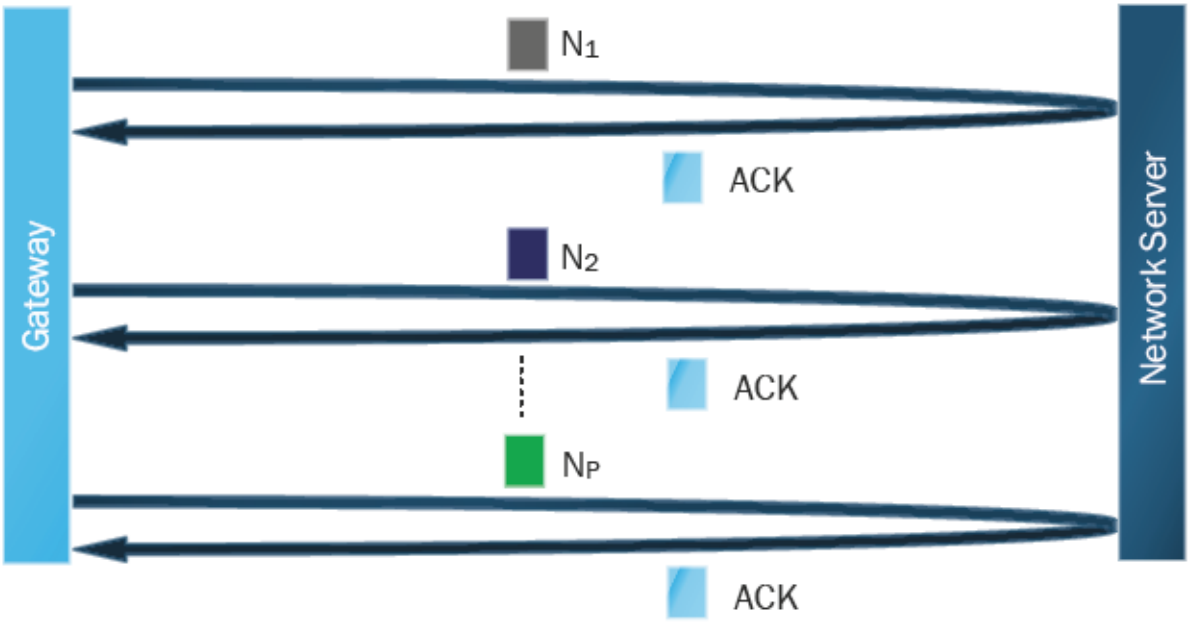

Figure 29. LoRaWAN gateway message forwarding protocol diagram.

In our work, the gateway aggregates the incoming small LoRa packets into one large packet to reduce the number of transmissions. After that, it transmits the several aggregated packets to NS through an IP network, and NS responds to it with single acknowledgement (ACK). To aggregate the incoming LoRa packets, gateway pays the delay cost of $W_q = \mu \times N_P$ seconds, then it transmits all of the aggregated packets in one transmission. The aggregation results into enhancement of goodput and considerably reduces the overhead of the transmission. Conversely, in traditional upstream message flow, the NS responds to every individual packet with an ACK message that wastes resources and takes extra overhead. Moreover, a UDP uplink transmission takes 8 bytes for UDP and 20 bytes for IP header, thus the fixed overhead is 28 bytes [64]. For instance, transmission of 61 packets will waste 1708 bytes of overhead. To eliminate this issue, our aggregation scheme suggests to transmit N_P aggregated packets at the overhead cost of only 28 bytes. Figure 30 presents a simplified general LoRaWAN network architecture for our proposed packet aggregation approach. Similarly, for illustration, Figure 31 shows the gateway message forwarding scheme with the aggregation mechanism.

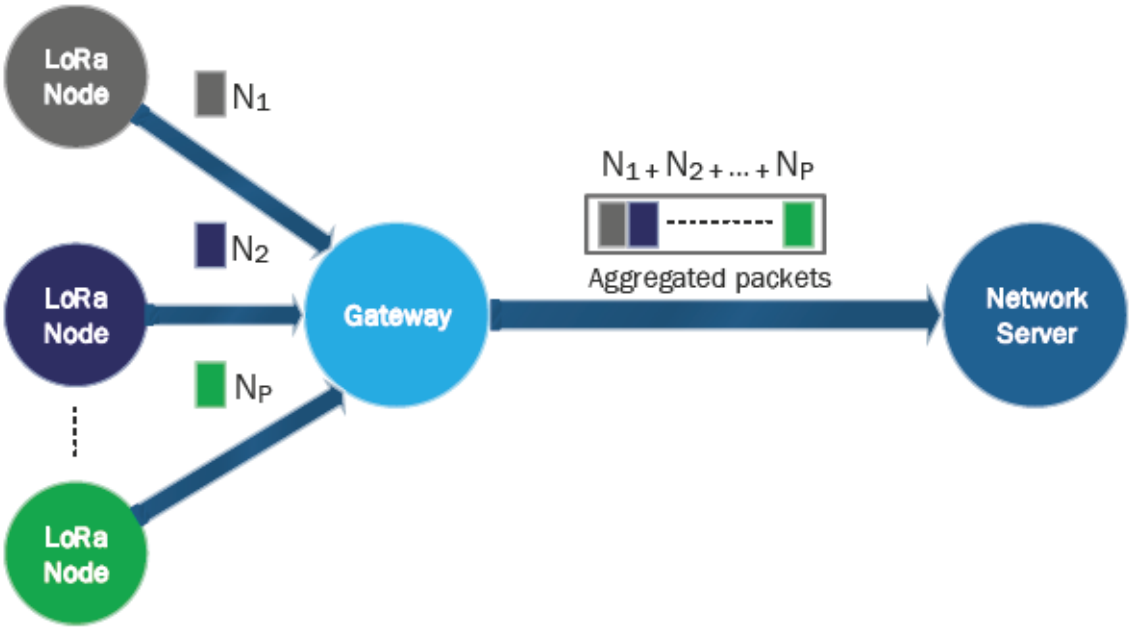

Figure 30. The network architecture for LoRa packet aggregation.

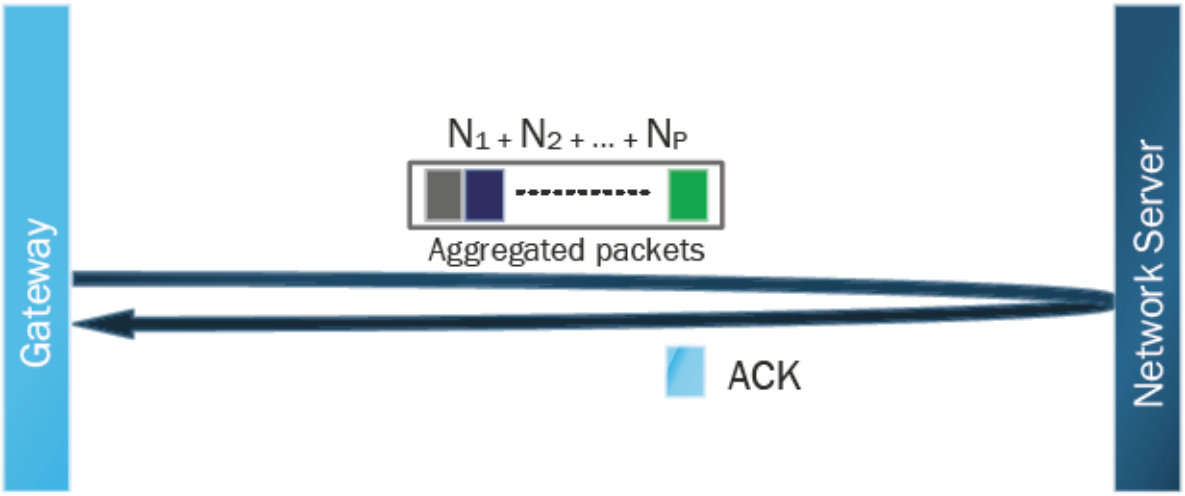

Figure 31. Aggregated LoRaWAN gateway message forwarding protocol diagram.

A consequence of proposed scheme is that the aggregation process causes queuing delay, thus in case of low traffic - time needed to fill the buffer might be huge, introducing a huge delay. However, for the massive connectivity scenario where the the mean inter-arrival time of packet arrivals at gateway is low, the aggregation process will be shorter and it will significantly reduce the overhead of the transmissions. Figure 32 illustrates the aggregation cost in terms of queuing delay for different traffic arrivals such as $\mu = [1, 2.7, 4.2, 6, 8]$ seconds. This way we can compare the cost of proposed aggregation mechanism with different scenarios of traffic arrivals.

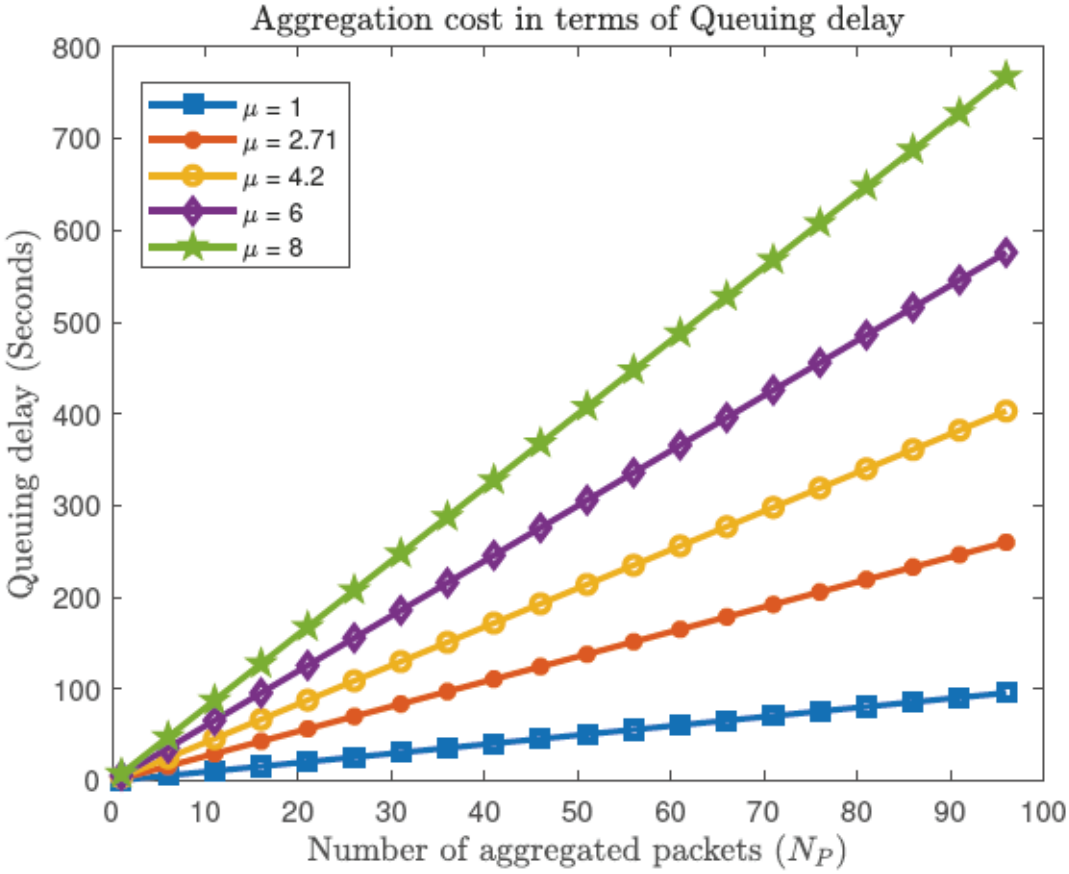

Figure 32. Aggregation cost in terms of queuing delay for high, medium and low traffic arrival rates $(1/\mu)$ at gateway.

4.4.1 Compatibility with LoRaWAN's downlink

It is very important to consider the compatibility of proposed aggregation solution for downlink transmissions. In typical LoRaWAN downlink communication, the NS has to have the possibility to send a downlink packet to sensor nodes within the offset time (RECEIVE_DELAY1) of the receive window (RX1). In case, if the aggregation period is longer than the RECEIVE_DELAY1 - the downlink communication will not work. This is a complex problem and a possible attractive solution to issue can be a multi-user ACK aggregation approach. The authors in [65], contributes by a novel ACK aggregation scheme for multiple users under duty-cycle restrictions. NS request the sensor nodes to active their receive windows synchronously so after that NS transmits the cumulative ACKs to multiple nodes at the same time. According to ACK-aggregation scheme, the node will wait for a long period before it sends the next data packet. The majority of LoRaWAN applications not concern about the delay because a node have to wait for next transmission due to duty-cycle restrictions. Figure 33 shows the overview of a multi-user ACK aggregation approach for LoRaWAN.

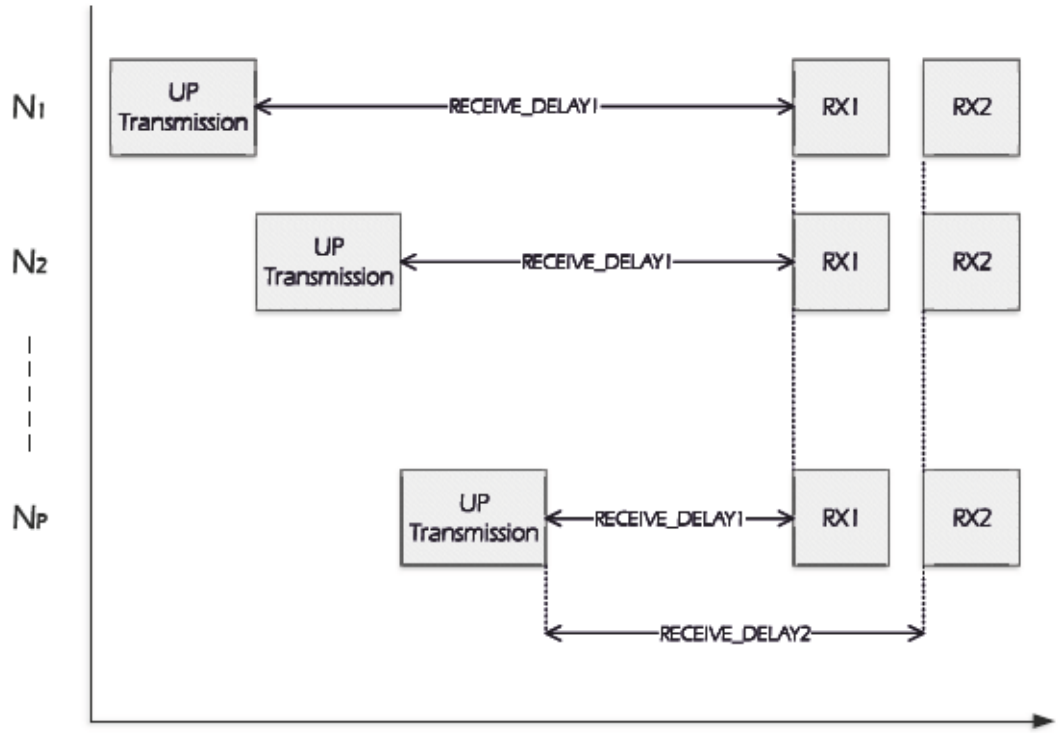

Figure 33. An overview of multi-user ACK aggregation mechanism.

Their performance analysis and simulation results show that ACK aggregation not only enhance the throughput but also improve the reliability of the data. They adopted ALOHA as collision model and the throughput is defined as

$$S_{Pure} = A \times e^{-2 \times A}, \tag{17}$$

where S_{Pure} is throughput and A is the rate of transmission-attempts per frame-time. At higher traffic loads A, the throughput decreases to zero as almost all the packets will lost due to collision. The multi-user ACK aggregation technique reduces the number of ACK transmissions that benefits in terms of higher throughput.

4.4.2 Goodput analysis

In 5GTN, the payload (P_L) of a LoRa packet is 24 bytes. As illustrated in Figure 28, the payload is 1500 bytes, it uses of which 8 bytes for UDP header and 20 bytes for IPv4 header, so remaining 1472 bytes are available for sending data per packet. Apart from it, overhead (H) of MAC destination and source address, optional 802.1q tag, length/type and CRC are 22 bytes long. We examine the goodput of system as a function of different number of aggregated packets. The mathematical expression to calculate the goodput is defined as

$$G = \frac{N_P \times P_L \times \left(1 - \epsilon\right)}{\left(N_P \times P_L + H\right) \times \frac{1}{\left(1-\epsilon\right)}}, \tag{18}$$

where ϵ is outage probability of the UDP channel, in our scenario we considered it as 10^{-5} bit-error rate. We analyse the system goodput as a function of number of aggregated packets ranging from N_P=1 to $N_PMax = \frac{1472}{24} = 61$ and the results are demonstrated in Figure 34.

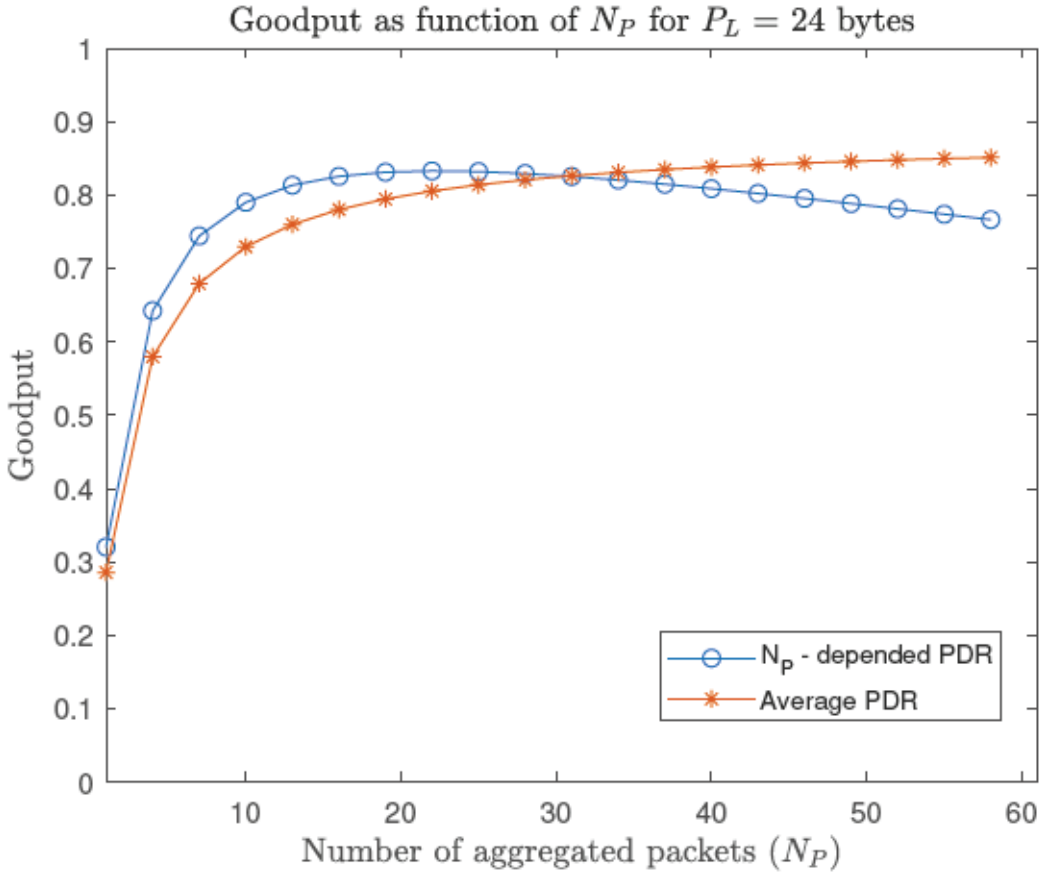

Figure 34. Goodput for N_P depended and averaged PDR as a function of number of aggregated packets for P_L=24.

Initially, the N_P dependent PDR starts from 0.3205 and increases dramatically until it reaches to 0.8328 at optimal point $N_{P^\star} = 22$. After that, it gradually decreases to 0.7589 at $N_P = 61$. On the other hand, in averaged PDR case, we average the $(1-\epsilon)$ to calculate the goodput by (18). The averaged PDR based goodput overtook N_P dependent PDR at $N_P = 31$ and kept growing slightly to max value of 0.8526 at $N_P = 61$.

The analysis is further narrowed down to lower payload of $P_L = 12$ bytes to observe the impact of payload on the network goodput. As expected, the maximum number of aggregated packets reaches to $N_PMax = \frac{1472}{12} = 122$, which are double the previous case. Figure 35 demonstrates the goodput as a function of aggregated packets with $P_L = 12$. In this scenario, the N_P dependent PDR is 0.1916 without aggregation, it raise to 0.3205 for $N_P = 2$. The trend of growth continues until it reaches to maximum PDR of 0.8328 at optimal $N_{P^\star} = 44$. After that, it declines steadily and touches the PDR of 0.7589 at $N_P = 122$. In both of the playload cases P_L=24 bytes and 12 bytes, the system experience maximum achievable value of 0.8328 at $N_P = 22$ and 44, respectively.

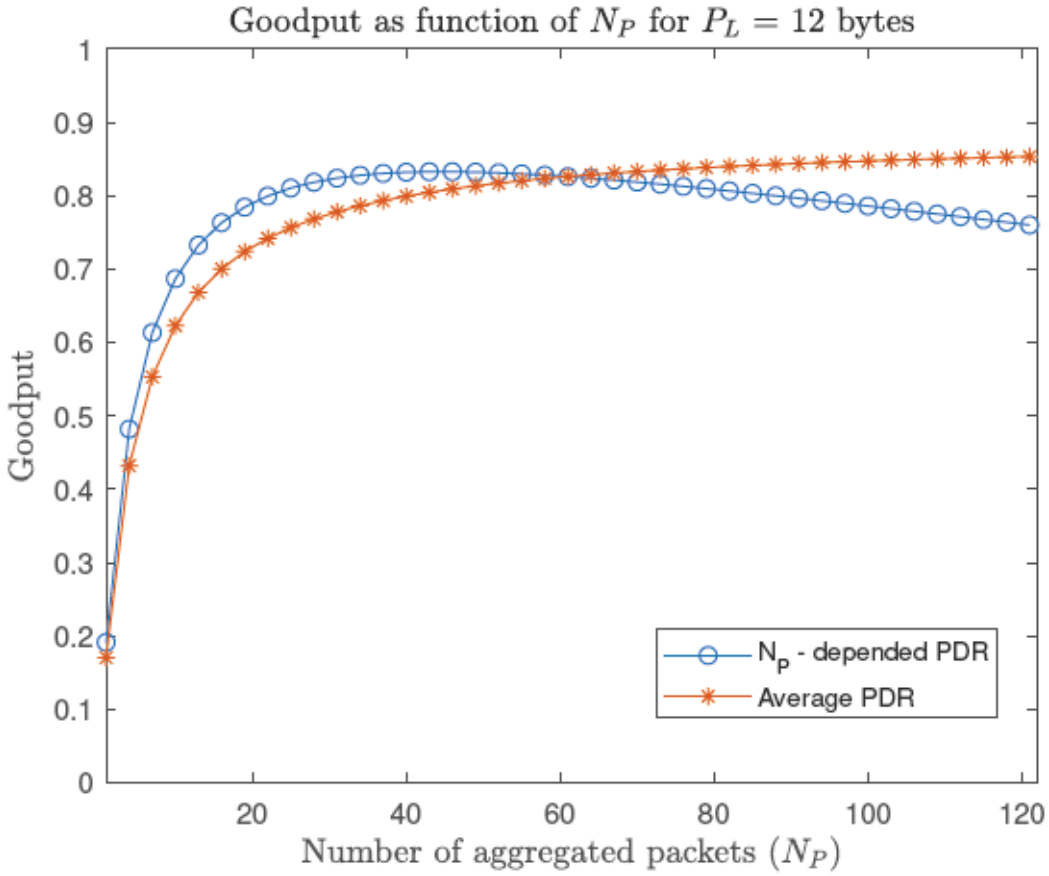

Figure 35. Goodput for N_P depended and averaged PDR as a function of number of aggregated packets for P_L=12.

We find the optimal $N_{P^\star}$ for different size of payloads ranging from 18 bytes to 72 bytes. The mathematical expression of optimal $N_{P^\star}$ is given as

$$N_{P^\star} = \max_{N_P} \; G(N_P), \tag{19}$$

As expected, the result illustrates that the number of aggregated optimal $N_{P^\star}$ decrease by increasing the payload size. In Figure 36 payload, optimal $N_{P^\star}$, and goodput relation depicts that the goodput remains constant 0.8328 at any optimal $N_{P^\star}$ for a given payload.

It is important to noting that, the traffic aggregation is beneficial to save resources and bandwidth. Conventionally, the LoRaWAN message forwarding protocol transmits a single packet at a time using unslotted ALOHA. As we know, ALOHA networks have a high collision probability. Our work shows the positive impact of aggregation at the system goodput. The aggregation mechanism reduces the number of transmissions that will also help to decline the collisions in the network.

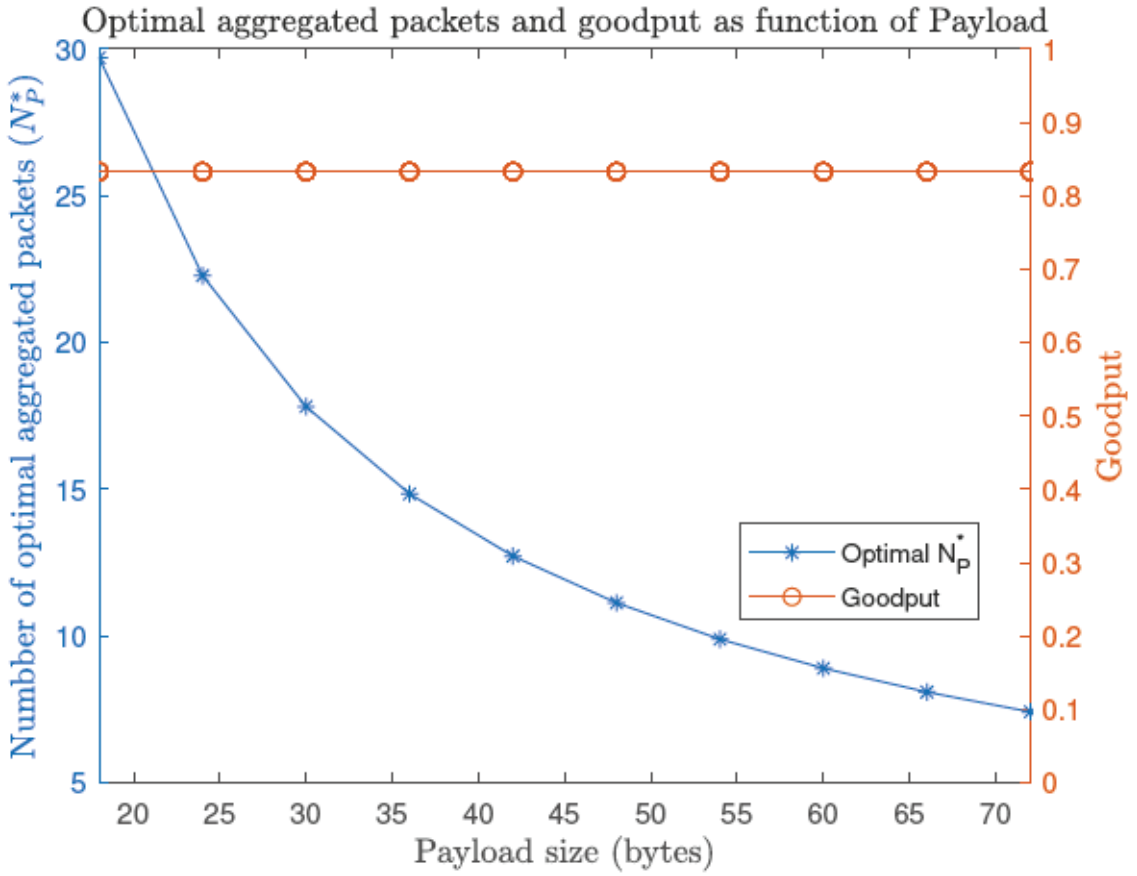

Figure 36. Number of optimal aggregated packets (N_{P^*}) and system goodput as a function of payload (P_L) ranging from 18 to 72 bytes of the individual devices' messages.

4.5 Discussion

Network statistical characteristics analysis are the basic fundamental to deeply understand the influence of IoT applications for the traffic modeling and optimization of a network. This thesis work presents the characteristics of aggregated traffic in LoRaWAN and proposes a approach for the optimization of gateway to NS packet forwarding protocol. Unlike the typical upstream message flow, proposed mechanism aggregates the LoRa packets up to N_P, after that gateway transmits these aggregated packets in single transmission and reduces the overhead at the cost of queuing delay. For instance, to transmit N_P aggregated packets the queuing delay at gateway will be $W_q = \mu \times N_P$ seconds. Table 6 shows the average measured, analytical and theoretical delays for different numbers of N_P. As we increase the N_P, it will also raise the goodput cost in terms of waiting delay. For the transmission of N_P=61, gateway will pay the average cost of $4.2 \times 61 = 256.2$ seconds. As an advantage, we are increasing the goodput of system from 0.3205 to 0.7589 for N_P=1 to N_P=61, respectively. The queuing delay also directly depends on traffic arrivals, in case of low incoming traffic at the gateway - the time needed to fill the buffer might be huge, introducing a larger delay. Unlike our context, in real-world heterogeneous networks, the traffic characteristics are generally periodic, event-driven or streams different priorities which needs more intelligent solutions

for data aggregation. Another downside of proposed aggregation mechanism is the compatibility with the LoRaWAN downlink, typical NS deliver downlink data within the RECEIVE_DELAY1. In our scenario, aggregation period is longer than the conventional RECEIVE_DELAY1 that is why this approach is not suitable for downlink traffic. To solve the issue, ACKs aggregation schemes [65] can be used to enable downlink traffic.

In LoRaWAN, the nodes are not connected with a specific gateway. Instead, the packets transmitted by a nodes are generally received by multiple gateways and each of them is responsible to forward the received data to NS via an IP based network. NS manages the network and schedules ACK through the optimal gateway [66]. Considering the fact that nodes are connected with multiple gateways, the proposed packet aggregation scheme require more intelligence and functionalities to handle this complexity. This motivates us to extend our current work in future to the use case of multiple gateways.

Gateway to NS upstream message reliability is also a drawback of proposed aggregation mechanism. For the worst case scenario, if network loses one transmission of N_P=61 aggregated packets, it means that system will lose the data of 61 LoRa sensors. Application transferring few UDP packets per transaction will be unlikely to experience reliability issues. The big problem arises with use cases that needs a large number of of sequential UDP packets to complete a single transaction, for instance TFTP for file transfer [64]. Let us consider an application scenario where the multiple gateways share the common medium to communicate with NS. In such use cases, our aggregation mechanism will not only reduce the number of transmissions and overhead on the gateway to NS link but could also decrease the collision probability.

5 CONCLUSION

This work focused on statistical characteristics analysis of 5GTN LoRaWAN traffic, and also modeled the aggregated traffic. Our 5GTN LoRaWAN data analysis showed that the traffic behaviour is exponential and most of transmissions were made within a inter-arrival time of 10 seconds. In particular, we examine the traffic for different weeks, busiest and lightest day, similarly for different hours of the day. Finally, from the statistical analysis we concluded that the average inter-arrival time is between 4.1 to 4.2 seconds. To achieve the goal of 5GTN LoRaWAN aggregated traffic modeling, we fitted the intervals of the received packets into exponential distribution that further helped us to model the traffic. To verify the aggregated model, we compared the delay of our model with the actual delay of 5GTN traffic data set for different number of packets $N_P = 1$, 10, 30, and 60. The results verified that our analytical analysis matched with the data set. So far most of the conventional IoT traffic models are based on assumptions, considering that the arrival of data is either standard poisson or exponential distribution. Our work overcome this problem, we presented an accurate model of real-life large-dense LoRaWAN deployment consisting of 331 sensors.

Traditionally, LoRa gateway transmits a single packet to NS. In this thesis work, we proposed to transmit the aggregated packets and results illustrate that the system goodput increased from 0.3205 to 0.7589 by aggregating the packets from $N_P = 1$ to 61, respectively, by doing so we reduce N_P-fold the number of transmissions between gateway and NS assuming no retransmissions were required. Therefore, as we assume that gateway is connected to the NS, the proposed aggregation can potentially reduce the collisions and interference at the NS. Furthermore, we also calculated the optimal number of the aggregated packets for the different values of the payload. The results showed the maximum achievable good is 0.8328 for any given payload $18 \geq P_L \leq 72$ bytes. Further, we maximize the gateway to NS level system goodput by transmitting more LoRa packets to use resources efficiently. Future work, our plan is to model the aggregated traffic and perform optimization on multiple gateways scenarios with traffic prioritization.

6 REFERENCES

[1] Sisinni E., Saifullah A., Han S., Jennehag U. & Gidlund M. (2018) Industrial Internet of Things: Challenges, Opportunities, and Directions. IEEE Transactions on Industrial Informatics 14, pp. 4724–4734.

[2] Sotres P., Lanza J., Sánchez L., Santana J.R., López C. & Muñoz L. (2019) Breaking Vendors and City Locks through a Semantic-enabled Global Interoperable Internet-of-Things System: A Smart Parking Case. Sensors (Basel, Switzerland) 19, pp. 1 – 6.

[3] Rodrigues J.J.P.C., De Rezende Segundo D.B., Junqueira H.A., Sabino M.H., Prince R.M., Al-Muhtadi J. & De Albuquerque V.H.C. (2018) Enabling Technologies for the Internet of Health Things. IEEE Access 6, pp. 13129–13141.

[4] Pacheco J., Satam S., Hariri S., Grijalva C. & Berkenbrock H. (2016) Iot Security Development Framework for building trustworthy Smart car services. In: 2016 IEEE Conference on Intelligence and Security Informatics (ISI), pp. 237–242.

[5] Asadullah M. & Ullah K. (2017) Smart home automation system using Bluetooth technology. In: 2017 International Conference on Innovations in Electrical Engineering and Computational Technologies (ICIEECT), pp. 1–6.

[6] Wang Y., Saez B., Szczechowicz J., Ruisi J., Kraft T., Toscano S., Vacco Z. & Nicolas K. (2017) A smart campus internet of things framework. In: 2017 IEEE 8th Annual Ubiquitous Computing, Electronics and Mobile Communication Conference (UEMCON), pp. 498–503.

[7] Saha H.N., Mandal A. & Sinha A. (2017) Recent trends in the internet of things. 2017 IEEE 7th Annual Computing and Communication Workshop and Conference (CCWC) , pp. 1–4.

[8] Internet of Things (IoT) Connected Devices Installed Base Worldwide from 2015 to 2025 (in Billions) (accessed 16.12.2019). URL: `https://www.statista.com`.

[9] Chuah J.W. (2014) The Internet of Things: An overview and new perspectives in systems design. In: 2014 International Symposium on Integrated Circuits (ISIC), pp. 216–219.

[10] Mekki K., Bajic E., Chaxel F. & Meyer F. (2019) A comparative study of LPWAN technologies for large-scale IoT deployment. ICT Express 5, pp. 1 – 7.

[11] Haxhibeqiri J., Karaagac A., Van den Abeele F., Joseph W., Moerman I. & Hoebeke J. (2017) Lora indoor coverage and performance in an industrial environment: Case study. In: 2017 22nd IEEE International Conference on Emerging Technologies and Factory Automation (ETFA), pp. 1–8.

[12] Ballerini M., Polonelli T., Brunelli D., Magno M. & Benini L. (2019) Experimental Evaluation on NB-IoT and LoRaWAN for Industrial and IoT Applications. In: 2019 IEEE 17th International Conference on Industrial Informatics (INDIN), vol. 1, vol. 1, pp. 1729–1732.

[13] Mohammed N.A., Mansoor A.M. & Ahmad R.B. (2019) Mission-critical Machine-Type Communication: An Overview and Perspectives Towards 5G. IEEE Access 7, pp. 127198–127216.

[14] Muhammad I., Alcaraz López O.L., Alves H., Osorio D.P.M., Benitez Olivo E.E. & Latva-aho M. (2019) Adaptive Secure Rate Allocation via TAS/MRC under Multi-Antenna Eavesdroppers. In: 2019 16th International Symposium on Wireless Communication Systems (ISWCS), pp. 666–671.

[15] Soltanmohammadi E., Ghavami K. & Naraghi-Pour M. (2016) A Survey of Traffic Issues in Machine-to-Machine Communications Over LTE. IEEE Internet of Things Journal 3, pp. 865–884.

[16] Chen S., Ma R., Chen H., Zhang H., Meng W. & Liu J. (2017) Machine-to-machine Communications in Ultra-Dense Networks—A Survey. IEEE Communications Surveys Tutorials 19, pp. 1478–1503.

[17] Mehmood Y., Haider N., Imran M., Timm-Giel A. & Guizani M. (2017) M2m Communications in 5G: State-of-the-Art Architecture, Recent Advances, and Research Challenges. IEEE Communications Magazine 55, pp. 194–201.

[18] Alam M., Nielsen R.H. & Prasad N.R. (2013) The evolution of m2m into iot. In: 2013 First International Black Sea Conference on Communications and Networking (BlackSeaCom), pp. 112–115.

[19] Datta S.K. & Bonnet C. (2015) Internet of things and m2m communications as enablers of smart city initiatives. In: 2015 9th International Conference on Next Generation Mobile Applications, Services and Technologies, pp. 393–398.

[20] Al-Falahy N. & Alani O.Y. (2017) Technologies for 5G Networks: Challenges and Opportunities. IT Professional 19, pp. 12–20.

[21] Herlich M., Pfeiffenberger T., Du J.L. & Dorfinger P. (2018) Survey of Scenarios for Measurement of Reliable Wireless Communication in 5G. In: SAFECOMP Workshops.

[22] Tahaei H., Afifi F., Asemi A., Zaki F. & Anuar N.B. (2020) The rise of traffic classification in iot networks: A survey. Journal of Network and Computer Applications 154, p. 102538.

[23] Zhang J., Chen X., Xiang Y., Zhou W. & Wu J. (2015) Robust Network Traffic Classification. IEEE/ACM Transactions on Networking 23, pp. 1257–1270.

[24] Al Khater N. & Overill R.E. (2015) Network traffic classification techniques and challenges. In: 2015 Tenth International Conference on Digital Information Management (ICDIM), pp. 43–48.

[25] Mocnej J. (2018) Network Traffic Characteristics of the IoT Application Use Cases. Tech. rep., School of Engineering and Computer Science, Victoria University of Wellington.

[26] Massive IoT in the city (accessed 07.03.2020). URL: https://www.ericsson.com/en/mobility-report/articles/massive-iot-in-the-city.

[27] Yasmin R., Petäjäjärvi J., Mikhaylov K. & Pouttu A. (2018) Large and Dense LoRaWAN Deployment to Monitor Real Estate Conditions and Utilization Rate. In: 2018 IEEE 29th Annual International Symposium on Personal, Indoor and Mobile Radio Communications (PIMRC), pp. 1–6.

[28] Gupta V., Devar S.K., Kumar N.H. & Bagadi K.P. (2017) Modelling of IoT Traffic and Its Impact on LoRaWAN. In: GLOBECOM 2017 - 2017 IEEE Global Communications Conference, pp. 1–6.

[29] Metzger F., Hoßfeld T., Bauer A., Kounev S. & Heegaard P.E. (2019) Modeling of Aggregated IoT Traffic and Its Application to an IoT Cloud. Proceedings of the IEEE 107, pp. 679–694.

[30] Farooq M.O. & Pesch D. (2018) Evaluation of Multi-Gateway LoRaWAN with Different Data Traffic Models. In: 2018 IEEE 43rd Conference on Local Computer Networks (LCN), pp. 279–282.

[31] Majumdar C., Lopez-Benitez M. & Merchant S.N. (2019) Accurate Modelling of IoT Data Traffic Based on Weighted Sum of Distributions. In: ICC 2019 - 2019 IEEE International Conference on Communications (ICC), pp. 1–6.

[32] Dawy Z., Saad W., Ghosh A., Andrews J.G. & Yaacoub E. (2017) Toward Massive Machine Type Cellular Communications. IEEE Wireless Communications 24, pp. 120–128.

[33] Salam T., Rehman W.U. & Tao X. (2018) Cooperative Data Aggregation and Dynamic Resource Allocation for Massive Machine Type Communication. IEEE Access 6, pp. 4145–4158.

[34] AlQahtani S.A. (2017) Analysis and modelling of power consumption-aware priority-based scheduling for M2M data aggregation over long-term-evolution networks. IET Communications 11, pp. 177–184.

[35] Hoeller A., Souza R.D., Alcaraz López O.L., Alves H., de Noronha Neto M. & Brante G. (2018) Analysis and Performance Optimization of LoRa Networks With Time and Antenna Diversity. IEEE Access 6, pp. 32820–32829.

[36] Barro P.A., Zennaro M., Degila J. & Pietrosemoli E. (2019) A Smart Cities LoRaWAN Network Based on Autonomous Base Stations (BS) for Some Countries with Limited Internet Access. Future Internet 11.

[37] Coonjah I., Catherine P.C. & Soyjaudah K.M.S. (2015) Experimental performance comparison between TCP vs UDP tunnel using OpenVPN. In: 2015 International Conference on Computing, Communication and Security (ICCCS), pp. 1–5.

[38] LoRaWAN Network Server Demonstration: Gateway to Server Interface Definition (accessed 07.03.2020). URL: https://www.thethingsnetwork.org/forum/uploads/default/original/1X/4fbda86583605f4aa24dcedaab874ca5a1572825.pdf.

[39] Network Architecture (accessed 07.03.2020). URL: https://www.thethingsnetwork.org/docs/network/architecture.html.

[40] Mikhaylov K., Petrov V., Gupta R., Lema M.A., Galinina O., Andreev S., Koucheryavy Y., Valkama M., Pouttu A. & Dohler M. (2019) Energy Efficiency of Multi-Radio Massive Machine-Type Communication (MR-MMTC): Applications, Challenges, and Solutions. IEEE Communications Magazine 57, pp. 100–106.

[41] Vangelista L., Zanella A. & Zorzi M. (2015) Long-Range IoT Technologies: The Dawn of LoRa™. In: FABULOUS.

[42] Petajajarvi J., Mikhaylov K., Roivainen A., Hanninen T. & Pettissalo M. (2015) On the coverage of LPWANs: range evaluation and channel attenuation model for LoRa technology. In: 2015 14th International Conference on ITS Telecommunications (ITST), pp. 55–59.

[43] Mekki K., Bajic E., Chaxel F. & Meyer F. (2019) A comparative study of lpwan technologies for large-scale iot deployment. ICT Express 5, pp. 1 – 7.

[44] Lavric A., Petrariu A.I. & Popa V. (2019) Long Range SigFox Communication Protocol Scalability Analysis Under Large-Scale, High-Density Conditions. IEEE Access 7, pp. 35816–35825.

[45] RPMA Technology (accessed 16.12.2019). URL: https://www.ingenu.com/technology/rpma/.

[46] Weightless Specification (accessed 16.12.2019). URL: http://www.weightless.org/about/weightless-specification.

[47] Wang Y..E., Lin X., Adhikary A., Grovlen A., Sui Y., Blankenship Y., Bergman J. & Razaghi H.S. (2017) A Primer on 3GPP Narrowband Internet of Things. IEEE Communications Magazine 55, pp. 117–123.

[48] Ratasuk R., Mangalvedhe N., Zhang Y., Robert M. & Koskinen J. (2016) Overview of narrowband iot in lte rel-13. In: 2016 IEEE Conference on Standards for Communications and Networking (CSCN), pp. 1–7.

[49] Di Vincenzo V., Heusse M. & Tourancheau B. (2019) Improving downlink scalability in lorawan. In: ICC 2019 - 2019 IEEE International Conference on Communications (ICC), pp. 1–7.

[50] Lauridsen M., Vejlgaard B., Kovacs I.Z., Nguyen H. & Mogensen P. (2017) Interference Measurements in the European 868 MHz ISM Band with Focus on LoRa and SigFox. In: 2017 IEEE Wireless Communications and Networking Conference (WCNC), pp. 1–6.

[51] Hoeller A., Souza R.D., Alves H., Alcaraz López O.L., Montejo-Sánchez S. & Pellenz M.E. (2019) Optimum LoRaWAN Configuration Under Wi-SUN Interference. IEEE Access 7, pp. 170936–170948.

[52] An1200.22 lora™ modulation basics, rev. 2. semtech, 2015 (accessed 16.12.2019). URL: http://www.semtech.com/uploads/documents/an1200.22.pdf.

[53] Asad Ullah M., Iqbal J., Hoeller A., Souza R.D. & Alves H. (2019) K-means Spreading Factor Allocation for Large-Scale LoRa Networks. Sensors 19.

[54] SX1272/3/6/7/8: LoRa Modem (accessed 08.03.2020). URL: https://usermanual.wiki/Pdf/LoraDesignGuideSTD.1867307571/html.

[55] Ertürk M.A., Aydın M.A., Büyükakkaşlar M.T. & Evirgen H. (2019) A Survey on LoRaWAN Architecture, Protocol and Technologies. Future Internet 11.

[56] LoRa Alliance (accessed 16.12.2019). URL: http://www.lora-alliance.org.

[57] Casals L., Mir B., Vidal R. & Gomez C. (2017) Modeling the Energy Performance of LoRaWAN. Sensors 17.

[58] Popovski P., Trillingsgaard K.F., Simeone O. & Durisi G. (2018) 5g Wireless Network Slicing for eMBB, URLLC, and mMTC: A Communication-Theoretic View. IEEE Access 6, pp. 55765–55779.

[59] Hoeller A., Sant'Ana J., Markkula J., Mikhaylov K., Souza R. & Alves H. (2020), Beyond 5G Low-Power Wide-Area Networks: A LoRaWAN Suitability Study.

[60] Explore 5G features and performance in a controlled, real environment (accessed 16.12.2019). URL: https://5gtn.fi/technology/.

[61] ERS CO2 (accessed 16.12.2019). URL: https://www.elsys.se/shop/product/ers-co2.

[62] Yasmin R., Petäjäjärvi J., Mikhaylov K. & Pouttu A. (2017) On the integration of LoRaWAN with the 5G test network. In: 2017 IEEE 28th Annual International Symposium on Personal, Indoor, and Mobile Radio Communications (PIMRC), pp. 1–6.

[63] Yasmin R., Salminen M., Gilman E., Petäjäjärvi J., Mikhaylov K., Pakanen M., Niemelä A., Riekki J., Pirttikangas S. & Pouttu A. (2018) Combining IoT Deployment and Data Visualization: experiences within campus maintenance use-case. In: 2018 9th International Conference on the Network of the Future (NOF), pp. 101–105.

[64] Efficient Data Transfer Over Cellular Networks white paper (accessed 22.04.2020). URL: https://www.digi.com/pdf/wp_efficientdatatransfer.

[65] Hasegawa Y. & Suzuki K. (2019) A Multi-User ACK-Aggregation Method for Large-Scale Reliable LoRaWAN Service. In: ICC 2019 - 2019 IEEE International Conference on Communications (ICC), pp. 1–7.

[66] Technical Overview of LoRa and LoRaWAN (accessed 22.04.2020). URL: https://lora-alliance.org/resource-hub/what-lorawanr.